VISVESVARAYA TECHNOLOGICAL UNIVERSITY BELGAUM

PROJECT REPORT ON

"EFFECT OF BUILD PLATFORM THICKNESS ON PART QUALITY IN POWDER BED SINTERING PROCESS"

Submitted in partial fulfillment of the requirements for the award of

BACHELOR OF ENGINEERING IN MECHANICAL ENGINEERING

For the academic year 2019-2020

Submitted by:

SHRAVANI B NAG
1CR16ME072

THIMMAIAH K S
1CR16ME083

Project carried out at

INTERNAL GUIDE

Dr. Harish Babu
ASSOCIATE PROFFESOR
Department of Mechanical Engineering, CMRIT

EXTERNAL GUIDE

Dr. Nagesh B K
SCIENTIST 'S'
MERF Group
GTRE, DRDO

DEPARTMENT OF MECHANICAL ENGINEERING
CMR INSTITUTE OF TECHNOLOGY
132, AECS Layout, IT Park Road,
Bangalore-560037

VISVESVARAYA TECHNOLOGICAL UNIVERSITY BELGAUM

DEPARTMENT OF MECHANICAL ENGINEERING
CMR INSTITUTE OF TECHNOLOGY
132, AECS Layout, IT Park Road,
Bangalore-560037

CERTIFICATE

This is to certify that the internship report entitled **"EFFECT OF BUILD PLATFORM THICKNESS ON PART QUALITY IN POWDER BED SINTERING PROCESS"** has been successfully completed by **Ms. SHRAVANI B NAG** and **Mr. THIMMAIAH K S** bearing USN: **1CR16ME072** and **1CR16ME083** are bonafide student of VTU in partial fulfillment for the award of **BACHELOR OF ENGINEERING** in **MECHANICAL ENGINEERING** of the **VISVESVARAYA TECHNOLOGICAL UNIVERSITY**, Belgaum during the year 2019-2020. It is certified that corrections/suggestions indicated for internal assessment have been incorporated in the project report. The project report has been approved as it satisfies the academic requirements in respect of project work prescribed for the said degree.

Signature of Principal **Signature of HOD**

Signature of Internal Guide **Signature of External Guide**

VISVESVARAYA TECHNOLOGICAL UNIVERSITY BELGAUM

DEPARTMENT OF MECHANICAL ENGINEERING
CMR INSTITUTE OF TECHNOLOGY
132, AECS Layout, IT Park Road,
Bangalore-560037

DECLARATION

We, **SHRAVANI B NAG and THIMMAIAH K S** bearing USN: **1C16ME072** and **1CR16ME083** respectively**,** are bonafide student of **CMR Institute of Technology**, Bangalore, hereby declare that the project entitled, "**Effect of build platform on part quality in powder bed sintering process**" has been carried out at Bosch Limited, Bangalore, in partial fulfillment of the requirements for the award of **BACHELOR OF ENGINEERING** in **MECHANICAL ENGINEERING,** of the **VISVESVARAYA TECHNOLOGICAL UNIVERSITY**, Belgaum, during the year 2019-2020. The work done in this project report is original and has not been submitted for any other degree in any university.

Project Report

On

"EFFECT OF BUILD PLATFORM THICKNESS ON PART QUALITY IN POWDER BED SINTERING PROCESS"

By

SHRAVANI B NAG **1CR16ME072**

THIMMAIAH K S **1CR6ME083**

DEPARTMENT OF MECHANICAL ENGINEERING
CMR INSTITUTE OF TECHNOLOGY
BANGALORE

ABSTRACT

This study is aimed at understanding the effect of build platform thickness of the 316L stainless steel on the quality of the components fabricated by the EOSINT M280 Model by using INCO-718 powder material and the machine is governed by the principle of direct material laser sintering process.

Numerical simulations were carried out using ANSYS Additive Manufacturing module on Benchmark 3D CAD model that delivers unparalleled accuracy in predicting final shape of the printed part, layer-by-layer distortion and stress, optimal support structures, distortion-compensated STL files and potential blade crash. Then these simulations are validated with the experimental observations.

The 3D printed Benchmark model is measured using the XRD and white light 3D scanner which gives the accurate method to investigate the residual stress levels on the surface layers. Such that these analysis provide simpler routes to reduce residual stress and hence enhance the component.

ACKNOWLEDGEMENT

It is our proud privilege and duty to acknowledge the kind of help and guidance received from several people in preparation of this report. Apart from our own, the success of this report depends largely on the encouragement and guidelines of many others. It would have not been possible to prepare this report in this form without their valuable help, co- operation and guidance.

We would like to express our deep sense of gratitude to our Principal **Dr. Sanjay Jain**, CMR Institute of Technology College, Bangalore for his motivation and for creating an inspiring atmosphere in college by providing state of the art facilities for preparation and delivery of this report.

Our sincere thanks to **Dr. Vijayananda Kaup**, Head of Department of Mechanical Engineering, for his whole-hearted support in completion of this project.

We are highly indebted to our project guide Associate Prof. **Dr. Harish Babu,** for guiding and giving timely advices and suggestions in the successful completion of this project.

Our sincere thanks to Assistant Prof. **Mr. Prashant S Hatti,** project coordinator for having supported the work related to this project. We would like to thank **Dr. Nagesh B K,** scientist 'S', MERF group ,GTRE (DRDO) for his enormous support in completion of this project.

Last but not least, we would like to put forward our heartfelt acknowledgement to all our classmates, friends and all those who have directly or indirectly provided their overwhelming support during our project work and the development of this report.

CONTENTS

1. ABOUT THE ORGANIZATION

1.1 DRDO

Defence Research and Development Organisation (DRDO) was established in 1958 by amalagamating Defence Science Organisation and some of the technical development establishments. A separate Department of Defence Research and Development was formed in 1980 which now administers DRDO and its 50 laboratories/establishments. DDRO is currently directed by A.P.J. Abdul Kalam, who was previously director of the Defence Research and Development Laboratory (DRDL) responsible for India's missile development program.

The Department of Defence Research and Development formulates and executes programmes of scientific research, design and development in the fields of relevance to national security leading to the induction of new weapons, platforms and other equipments required by the Armed Forces. It also functions as the nodal agency for the execution of major development programmes of relevance to Defence through integration of research, development, testing and production facilities with the national scientific institutions, public sector undertakings and other agencies. It functions under the control of Scientific Advisor to Raksha Mantri who is also Secretary, Defence Research and Development.

Research and development activities at DRDO cover important demarcated disciplines like aeronautics, rockets and missiles, electronics and instrumentation, combat vehicles, engineering, naval systems, armament technology including explosives research, terrain research, advanced computing, artificial intelligence,robotics, works study, systems analysis and life sciences including high-altitude agriculture, physiology, food technology and nuclear medicine. In addition to undertaking research and development activities, DRDO also assists the Services by rendering technical advice regarding formulation of requirements, evaluation of systems to be acquired, fire and explosive safety and mathematical and statistical analysis of operational problems.

DRDO has made significant achievements in its efforts to meet the requirements of the three Services. The notable developmental successes include flight simulators for aircrafts, 68mm reusable rocket pod, brake parachute for fighter aircrafts, mini remotely piloted vehicle, light field gun, new family of light weight small arms systems, charge line mine clearing vehicle for safe passage of vehicles in battlefield and illuminating ammunitions for enhancing night fighting capabilities. Cluster weapon systems for fighter aircraft, naval mines, next generation bombs for high speed aircraft and low-level hombing,

mountain gun, 130 mm SP gun, low-level tracking radar Indra-I and II for Army and Air Force, light field artillery radar, battlefield surveillance

radar, secondary surveillance radar have also been achieved. Bridge layer-tank Kartik, military bridging systems capable of withstanding tank load, advanced ship sonar systems, advanced sonobuoys, naval decoys. naval simulators, torpedo launchers, advanced materials and composites for military applications and parallel processsing computer for aerodynamic computations have also been developed.

Several high-technology projects are in various stages of design and development. The main battle tank Arjun, incorporating state-of-art tank technologies with superior fire power, high mobility and excellent protecion has been developed. A limited number of tanks are being produced as pre-production series which are in final stages of evaluation by the Army.

A light combat aircraft which would be lighter than any other combat aircraft and would incorporate modern design concepts and several state-of-the art technologies, is under full scale engineering development.

The Integrated Guided Missile Development program is in progress. The program comprises of five missile systems: Prithvi - surface-to-surface tactical battlefield missile, Akash medium range surface-to-air - missile systems, Trishul -a short range surface-to-air missile and Nag - third generation anti-tank missile, and Agni, an intermediate range ballistic missile.

DRDO offers specialised training at its two premier training institutions called Institute of Armament Technology, Pune and Defence Institute of Work Study, Mussoorie. The courses at these institutions have been evolved primarily to meet the needs of DRDO, Department of Defence Production.

1.2 GTRE

Gas Turbine Research Centre (GTRC) took its birth at No.4 BRD Air Force Station, Kanpur in 1959 with 8 Engineers/Scientists and about 20 Technicians. First indigenously developed centrifugal type gas turbine engine of 1000 kg thrust was tested in 1961. GTRC was moved to Bangalore, brought under the banner of DRDO, and was re-named as Gas Turbine Research Establishment (GTRE) in November 1961.

Gas Turbine Research Establishment is one of the pioneering Research and Development Organizations under the Ministry of Defence, Government of India. The main charter of the Establishment is to design and develop gas-turbine engines for military applications, besides carrying out advanced research work in the area of gas-turbine sub-systems. In addition, the Establishment is

responsible for establishing the requisite computational, prototype manufacturing and test facilities for components and full-scale engine development. The Establishment has a strong team of over 845 personnel drawn from science and engineering which includes aeronautics, mechanical, electronics, computer science, materials science, applied mathematics, etc. and support services.

Principal achievements of Gas Turbine Research Establishment include:

- Design and development of India's "first centrifugal type 10kN thrust engine" between 1959-61.
- Design and development of a "1700K reheat system" for the Orpheus 703 engine to boost its power. The redesigned system was certified in 1973.
- Successful upgrade of the reheat system of the Orpheus 703 to 2000K.
- Improvement of the Orpheus 703 engine by replacing "the front subsonic compressor stage" with a "transonic compressor stage" to increase the "basic dry thrust" of the engine.
- Design and development of a "demonstrator" gas turbine engine—GTX 37-14U—for fighter aircraft. Performance trials commenced in 1977 and the "demonstrator phase" was completed in 1981. The GTX 37-14U was "configured" and "optimized" to build a "low by-pass ratio jet engine" for "multirole performance aircraft". This engine was dubbed GTX 37-14U B.

2. KAVERI ENGINE

2.1 HISTORY

GTRE is entrusted with the design and development of Kaveri Engine which is low bypass twin spool turbo fan engine of 80 kN thrust class. The engine incorporates flat rated characteristics to mitigate the thrust drop due to high ambient intake temperature and / or high forward speed. Twin lane full authority digital engine control with an adequate manual backup is a salient design feature of Kaveri Engine.

The Kaveri was originally intended to power production models of the HAL Tejas Light Combat Aircraft. The engine features a six-stage core high-pressure (HP) compressor with variable inlet guide vanes (IGVs), a three-stage low-pressure (LP) compressor with transonic blading, an annular combustion chamber, and cooled single-stage HP and LP turbines. The development model is fitted with an advanced convergent-divergent variable nozzle

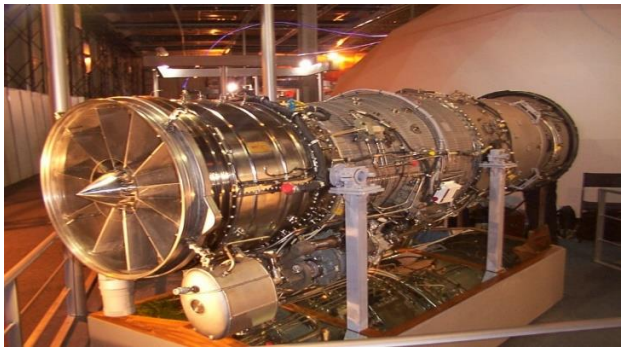

2.2 ASSEMBLY LINE OF ENGINE: The assembly line consists of modular assembly line, which is easier to replace if any part is damaged or failed. The assembly line manufactures KAVERI engine, which has sleek design and low bypass ratio, works on the principle of Brayton's cycle.

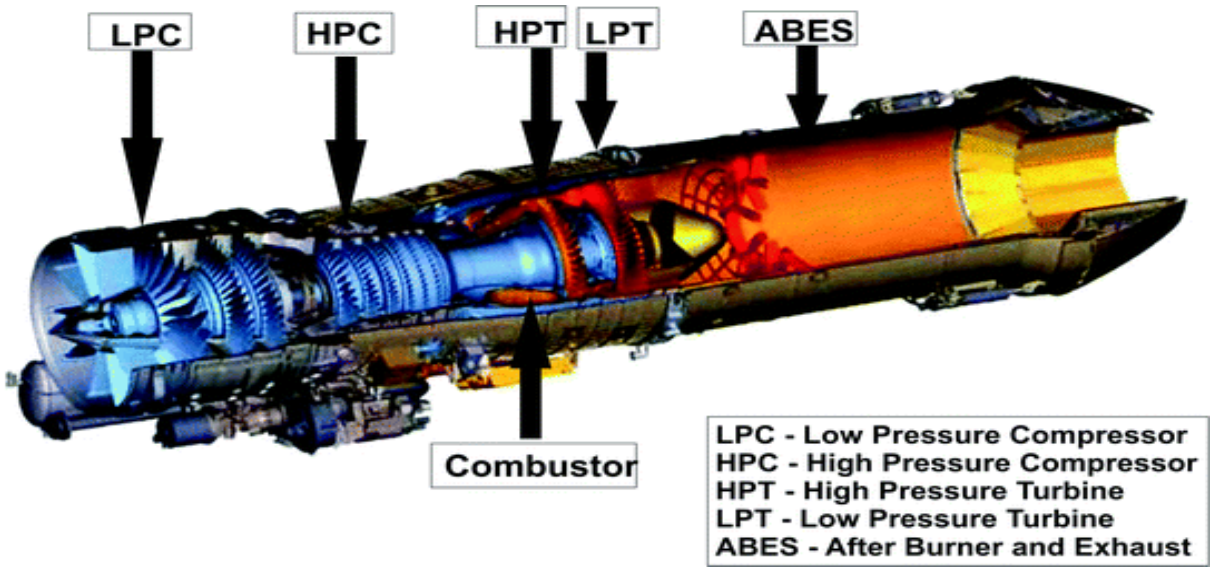

The engine features a six-stage core high-pressure (HP) compressor with variable inlet guide vanes (IGVs), a three-stage low-pressure (LP) compressor with transonic blading, an annular combustion chamber, and cooled single-stage HP and LP turbines. The development model is fitted with an advanced convergent-divergent variable nozzle.

2.3 SPECIFICATION

Length: 3,490.0 mm (137.4 in)

Diameter: 909.3 mm (35.8 in)

Dry weight: 1,236 kg (2,724 lb

Airflow:78 kg (172 lb) per second

Bypass ratio: 0.16:1

Overall pressure ratio: 21.5:1

LP compressor pressure ratio: 3.4:1

HP compressor pressure ratio: 6.4:1

.

2.4 PROBLEMS

The Kaveri program has attracted much criticism due to its ambitious objective, protracted development time, cost overruns, and the DRDO's lack of clarity and openness in admitting problems. Much of the criticism of the LCA program has been aimed at the Kaveri and Multi-Mode Radar programs. There has been much criticism of the degree of realism in the DRDO's planning schedules for various elements of the LCA programme, most particularly for the Kaveri development effort. France's SNECMA, with over half a century of successful jet engine development experience, took nearly 13 years to bring the Rafale fighter's M88 engine to low-volume production after bench testing had begun; a similar timespan for the less-experienced GTRE would see Kaveri production beginning no earlier than 2009. Another criticism has been DRDO's reluctance to admit problems in the engine and its resistance to involve foreign engine manufacturers until the problems became too large to handle.

In August 2010, regarding the reasons for delay, a Ministry of Defense press release reported:

1. "Ab-initio development of state-of-the-art gas turbine technologies.
2. Technical/technological complexities.
3. Lack of availability of critical equipment & materials and denial of technologies by the technologically advanced countries.
4. Lack of availability of test facilities in the country necessitating testing abroad.
5. Non availability of skilled/technically specialized manpower."

2.5 CURRENT STATUS

The DRDO currently hopes to have the Kaveri engine ready for use on the Tejas in the latter half of the 2010s decade and according to latest news still research on it is going on and the time to complete its research has been extended to 2011-2012.

"In recent times, the engine has been able to produce thrust of 18,000 lb_f (82 kN) but what the IAF and other stake-holders desire is power between 20,000–21,000 lb_f (90–95 kN)", senior officials told The Hindu. "On using the Kaveri for the LCA, they said the engine would be fitted on the first 40 LCAs to be supplied to the IAF when they come for upgrades to the DRDO in the latter half of the decade." Article further adds that in 2011, 50-60 test flights will be carried out to mature the engine in terms of reliability, safety and airworthiness.

India's Gas Turbine Research Establishment (GTRE) aims to integrate the Kaveri power-plant with the Hindustan Aeronautics Ltd (HAL) Tejas fighter within the next nine months. A test aircraft operated by India's Aeronautical Development Agency will be used for the integration, says an industry source familiar with the programme. If the integration is successful, the GTRE hopes to see a Tejas fly with a Kaveri power-plant by the end of 2013.

In Lok Sabha on 10 December. 2012 Defence Minister A K Antony gave an update on the progress made by the Kaveri Engine Development Project as follows:

1. So far, 9 prototypes of Kaveri Engine and 4 prototypes of Kabani (Core) Engine have been developed.
2. 2,200 hours of test (ground and altitude conditions) has been conducted.
3. The following two major milestones have been achieved:
1. Successful completion of Official Altitude Testing (OAT) ; and
2. Demonstration of First Block of flight of Kaveri Engine in Flying Test Bed (FTB).

Kaveri Engine was integrated with IL-76 Aircraft at Gromov Flight Research Institute (GFRI), Russia and flight test was successfully carried out up to 12 km (39,000 ft) maximum altitude and maximum forward speed of 0.7 Mach. Twenty Seven flights for 57 hours duration have been completed.

DRDO demonstrated its technological capability in aero-engine technology. This has been a great achievement in the aerospace community of the country, when the first ever indigenously developed fighter aircraft engine was subjected to flight testing. Tacit knowledge acquired by the DRDO scientists during this project will also be applied for further aerospace technology. Kaveri spin-off engine can be used as propulsion system for Indian Unmanned Strike Air Vehicle (USAV).

In January 2013, the GTRE director said that they are abandoning the plan for co-development with Snecma, but they still need an overseas partner, which will be selected through competitive bidding.

In November 2014, The Defense Research and Development Organization (DRDO) decided to abandon the Kaveri engine (GTX-35VS) programme due to its shortcomings.

2.6 APPLICATIONS

Plans are also already under way for derivatives of the Kaveri, including a non-afterburning version for an advanced jet trainer and a high-bypass-ratio turbofan based on the Kaveri core, named as Kabini

- GTX-35VS Kaveri:
  - HAL Tejas (planned for production models)
  - HAL Advanced Medium Combat Aircraft
- Derivatives:
  - Kaveri Marine Gas Turbine (KMGT), a recently developed derivative of the GTX-35VS Kaveri engine for ships.
  - Ghatak, a Kaveri derivative to be developed to power India's Unmanned Combat Air Vehicle DRDO AURA.

3.RECENT DEVELOPMENTS

Initial sanction for the development of GTX-35-VS was given in 1989 and christened as KAVERI engine in the first meeting of Aero Engine Development Board. Three full engines and two core engines were successfully tested to prove the concept.

With redesigned compressor, six full engines and one core engine were built and successfully tested at altitude conditions and the performance evaluated. The marine version of this engine for the Navy was conceived and the first prototype was successfully integrated and tested at Naval Dockyard, Visakhapatnam.

73 hours of Altitude Testing was conducted at Central Institute of Aviation Motors (CIAM), Russia in 2009-10 and the performance and operability of the engine were verified. 57 hours of Flight Tests were completed in IL-76 aircraft at Russia covering altitude up to 12 km and Mach No. 0.7 in 2010-11. About 3000 hours of testing completed at ground and altitude conditions as on date. GTRE is an ISO 9001:2015 certified establishmet.

4. AIRCRAFT ENGINES

4.1 Basic Engine Theory

Newton's third law of motion states that for every action there is an equal and opposite reaction. If you have ever fired a shotgun and felt the recoil, you have experienced an example of action-reaction (fig: 2.1). This law of motion is demonstrated in a gas turbine by hot and expanding gases striking the turbine wheel (action) and causing the wheel to rotate (reaction).

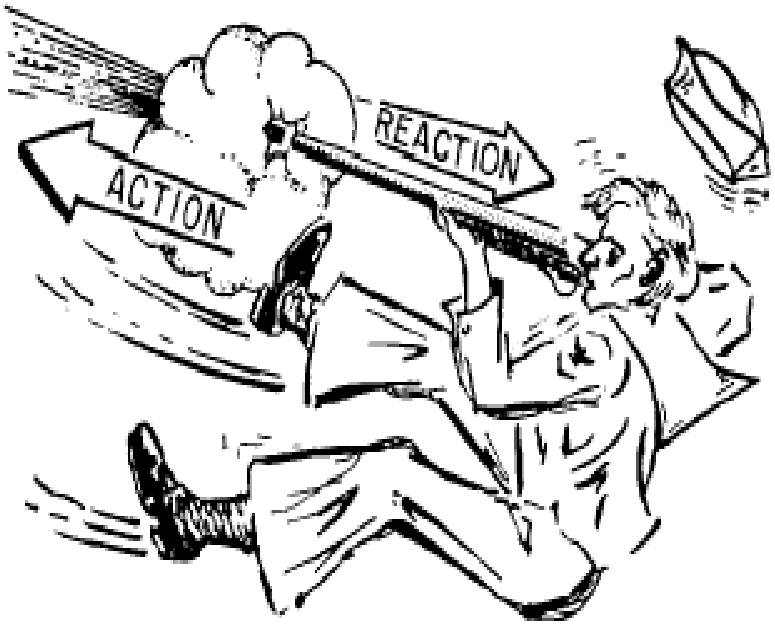

Figure 1: Newton's Third Law of Motion

4.1.1 Operating Principles

Figure 2 demonstrates the basic principles of gas turbine operation. A blown-up balloon (fig: 2, view A) does nothing until the trapped air is released. The air escaping rearward (fig: 2, view B) causes the balloon to move forward (Newton's third law). If we could keep the balloon full of air (fig: 2, view C), the balloon would continue to move forward. If a fan or pinwheel is placed in the air stream (fig: 2, view D), the pressure energy and velocity energy will rotate the fan and it can then be used to do work.

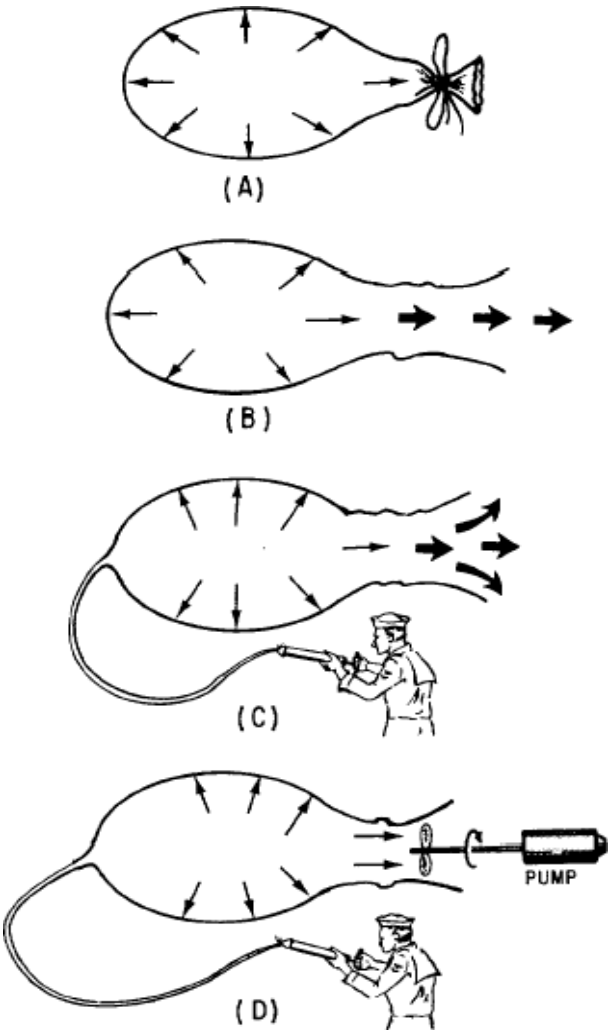

Figure 2: Turbine operating theory.

By replacing the balloon with a stationary tube or container and filling the tube with air from a fan or series of fans, we can use the discharge air to do work by turning a fan at the rear of the tube (fig: 3, view A). If fuel is added and combustion occurs, we greatly increase both the volume of air and the velocity that propels it over the fan. This increases the horsepower the fan will produce (fig: 3, view B). The continuous pressure created by the inlet fan, or compressor, prevents the hot gases from going forward. Next, if we attach a shaft to the compressor and extend it back to a turbine wheel, we have a simple gas turbine. It can supply power to run its own compressor and still provide enough power to do useful work, such as to drive a generator or propel a ship (fig: 3, view A). By comparing view A with view B in fig: 4, you can see that a gas turbine is very similar to our balloon turbine.

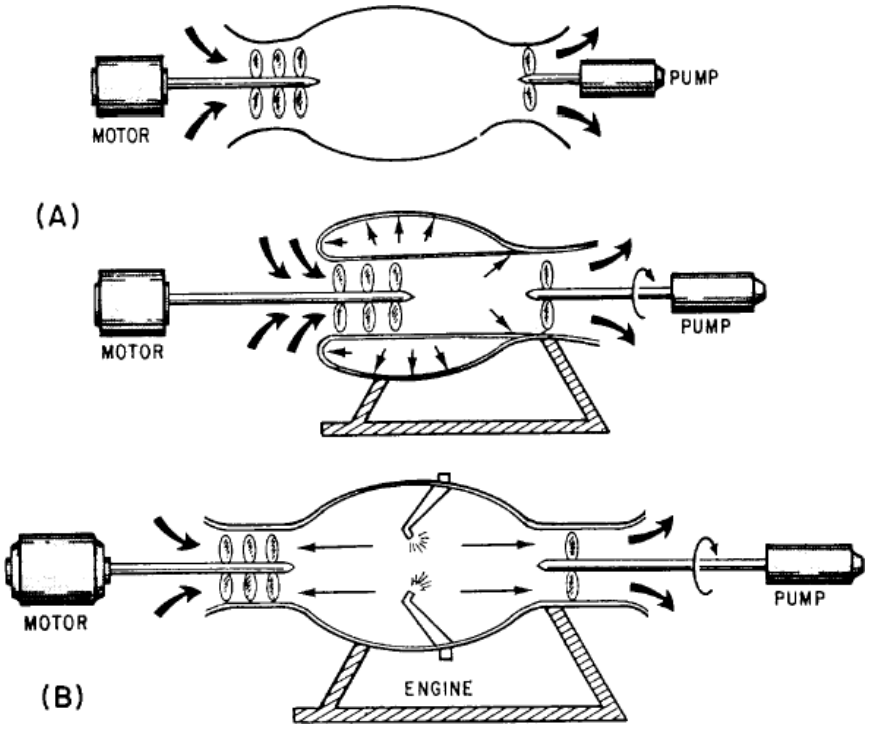

Figure 3: Turbine operating theory

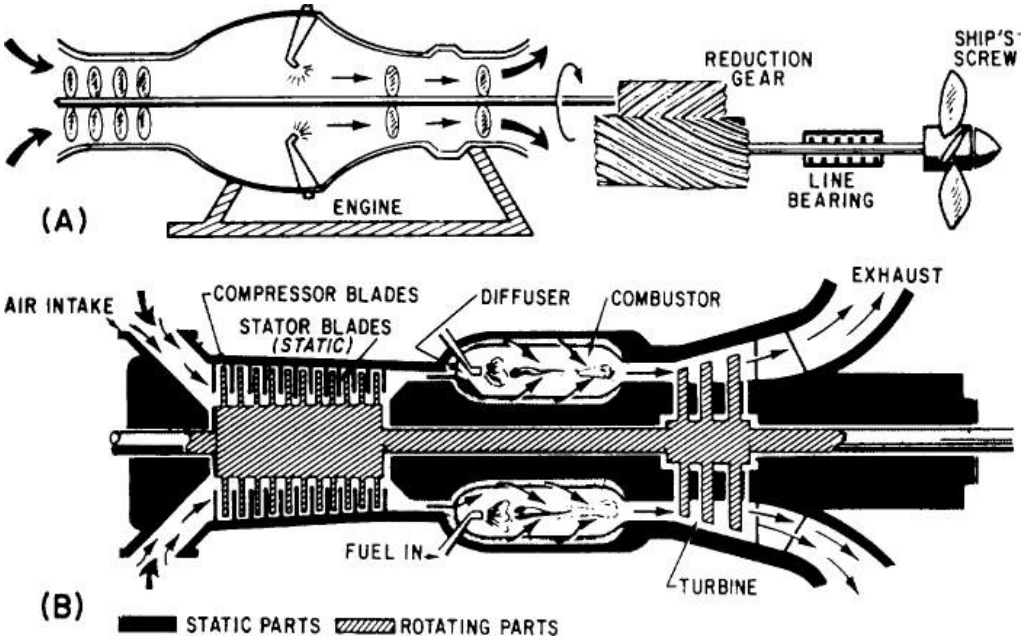

Figure 4: Practical demonstration of turbine operating theory

4.2 Classification of Aircraft Engines

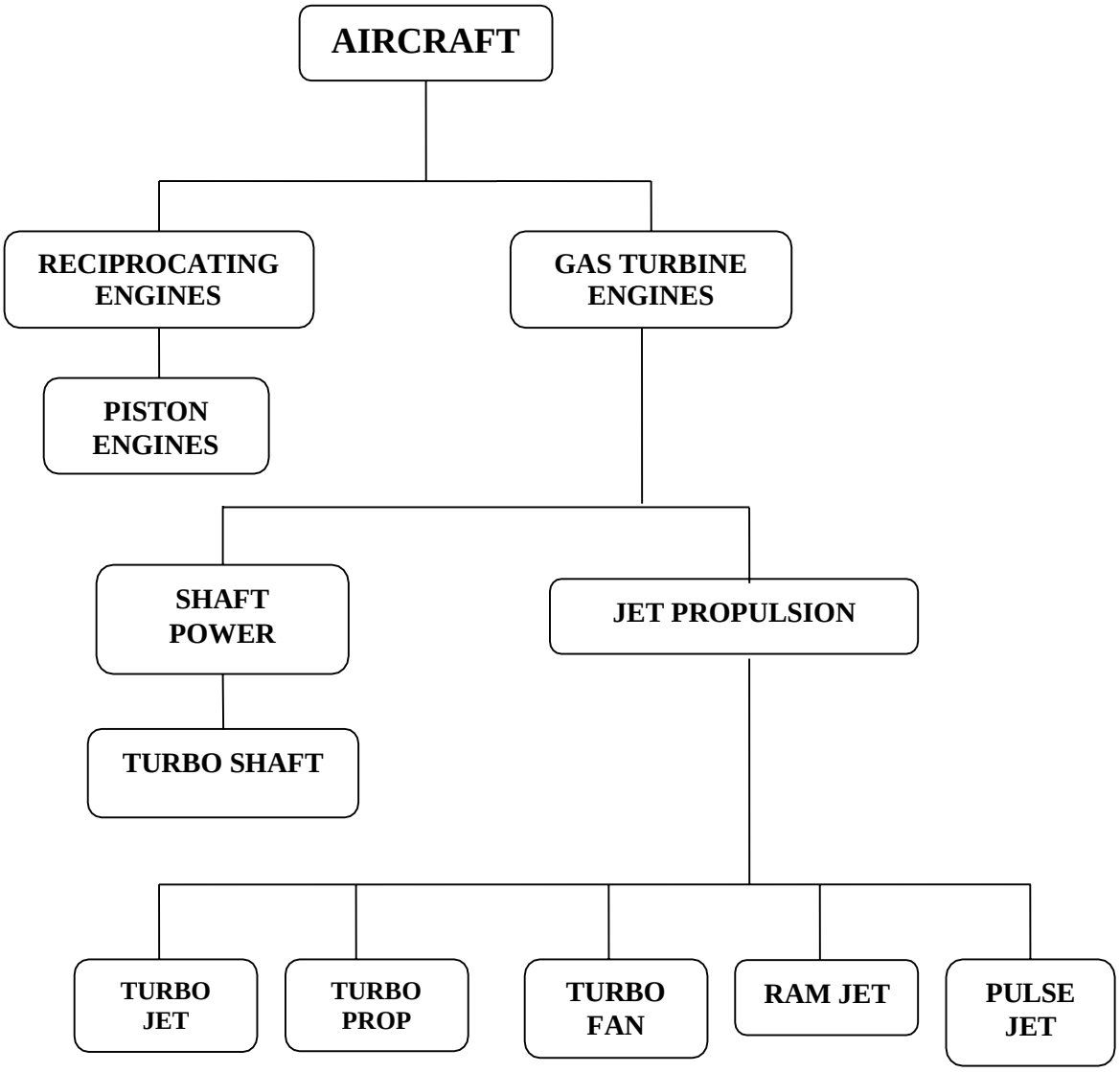

Figure 5: Classification of Aircraft Engines

4.3 Gas Turbine Engines

Mechanical power is most satisfactorily generated in a gas turbine which has the advantage of reliability, reduced vibration and the ability to produce large power output from units of smaller size and weight. The basic components of every gas turbine engine are:

- Compressor.
- Combustion Chamber (Burner).
- Turbine Assembly.

A Gas Turbine Engine is essentially a heat engine using air as the working medium to provide the required thrust. To achieve this, the air passing through the engine has to be accelerated. First, the Pressure Energy is raised by passing through the compressor followed by addition of Heat Energy by the combustion of fuel and then the final conversion to Kinetic Energy in the form of high jet velocity.

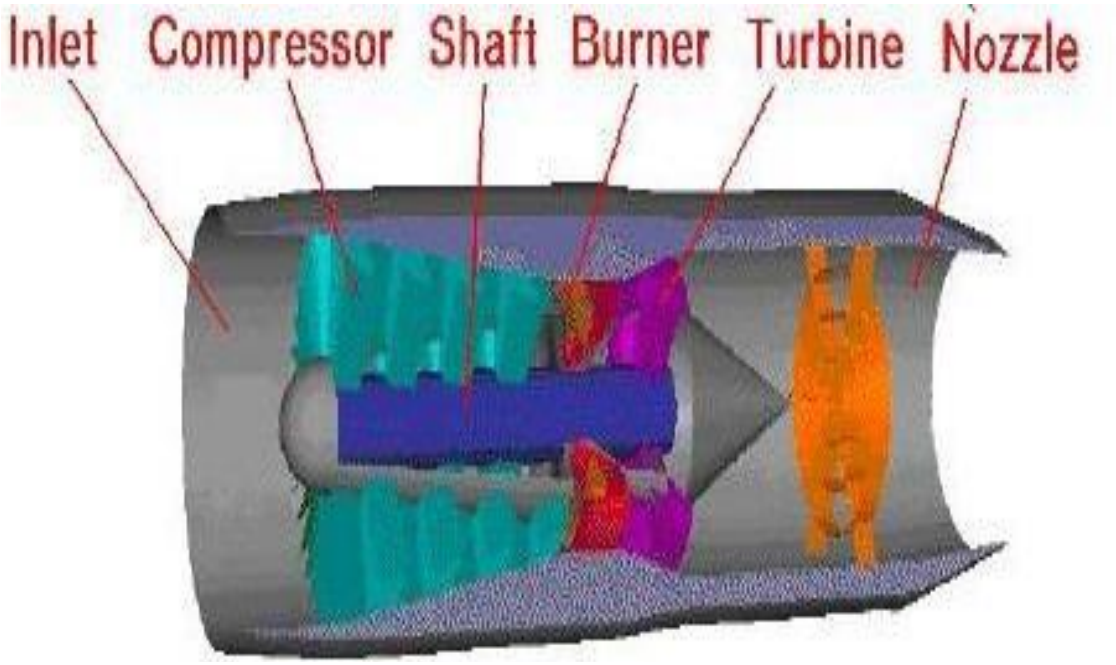

Figure 5: sectional view of a gas turbine engine

4.3.1 Types of Gas Turbines

Gas Turbine Engines are broadly classified into 4 types namely:

- Turbo shaft engines
- Turbo prop engines
- Turbo fan engines
- Turbojet engines

- **Turbo Shaft Engines**

In a Turbo Shaft Engine, the air intake is generally of regular cross section and therefore there is nearly no transformation for the turbo shaft engines. In these engines the air intake is often provided with protective guard or a sand filter. The power of the engine is received at the output shaft which is then coupled to the rotor in the case of helicopters.

Figure 6: sectional view of turbo shaft engine

- **Turbo Prop Engines**

In a Turbo Prop Engine, the air intake is generally located behind the propeller and therefore the propeller improves the capture of air. The expansion of gases takes place partly in the turbine and partly in the nozzle. The power developed by the turbine is consumed in running the compressor and propeller. The propeller motion and jet produced by the nozzle provide the thrust for the forward motion of the aircraft.

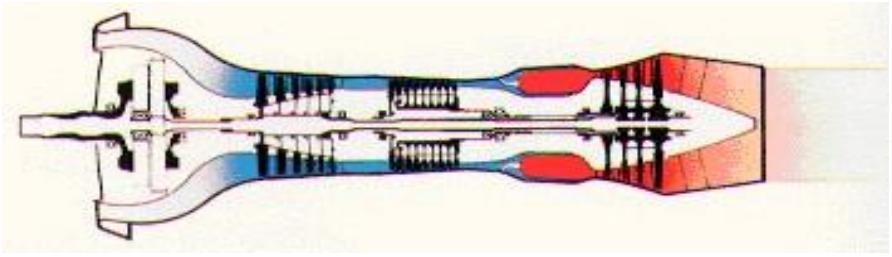

Figure 7: sectional view of turbo prop engine

- ## Turbo Fan Engines

A Turbo Fan Engine has a duct enclosed fan mounted at the front of the engine and driven either mechanical geared down or at the same speed as the compressor or by an independent turbine located either at the rear of the compressor or at the rear of the compressor drive turbine. In such engines the air intake is divergent in order to transform part of the Kinetic Energy of the air into Pressure Energy.

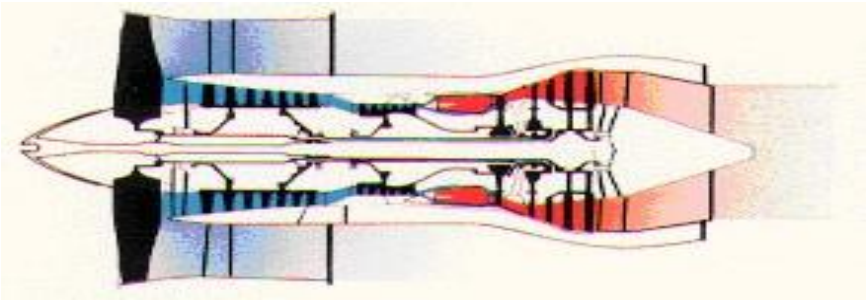

Figure 8: sectional view of turbo fan engine

The exhaust gases from the gas turbine which are at a high pressure than the atmospheric pressure is expanded in a nozzle and a very high velocity jet is produced which provides the thrust required for the forward motion of the aircraft. Turbo Fan Engines have a high propulsion efficiency.

- **Turbo Jet Engines**

The basic idea of the turbojet engine is simple. Air taken in from an opening in the front of the engine is compressed to 3 to 12 times its original pressure in a compressor. Fuel is added to the air and burned in a combustion chamber to raise the temperature of the fluid mixture to about 1,100°F to 1,300° F. The resulting hot air is passed through a turbine, which drives the compressor. If the turbine and compressor are efficient, the pressure at the turbine discharge will be nearly twice the atmospheric pressure, and this excess pressure is sent to the nozzle to produce a high-velocity stream of gas which produces a thrust. Substantial increases in thrust can be obtained by employing an afterburner. The afterburner increases the temperature of the gas ahead of the nozzle. The result of this increase in temperature is an increase of about 40 percent in thrust at takeoff and a much r percentage at high speeds once the plane is in the air.

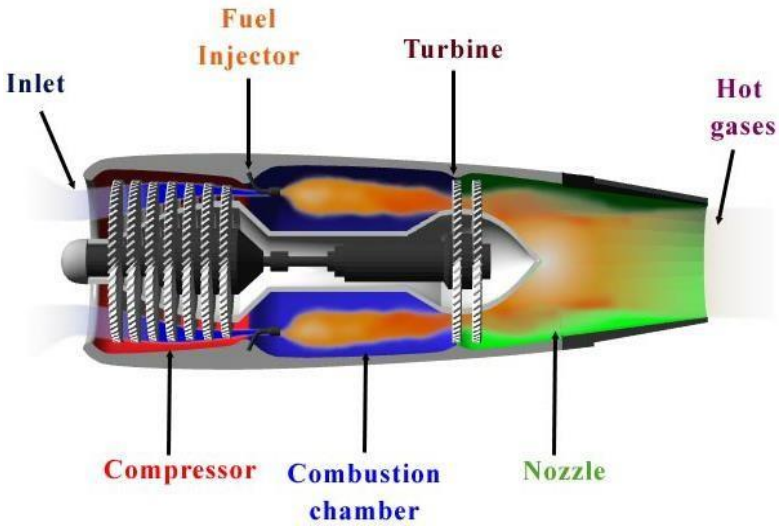

Figure 9: sectional view of turbo jet

5.ANALYSIS ON BUILD PLATFORMS

5.1 Case Studies

5.1.1 Effect of build location on microstructural characteristics and corrosion behavior of EB-PBF built Alloy 718

Alloy 718 are investigated to issue recommendations to the designers. It was found that the gap between the samples and height from the build plate affect the microstructural characteristics such as Nb-rich phase fraction and level of defects. However, the influence of the sample location due to a limited number of manufactured samples on the build plate did not show a clear trend. Similar to the effects of the gap between the samples and the height from the build plate on the microstructure, it is assumed that the part location shows similar behavior on the microstructure. There is a hypothesis that the innermost region (defined as “interior region”) of the build space is warmer, and the temperature radially decreases towards the outermost region (defined as “exterior region”). It can, therefore, be expected that parts built in the exterior region have a finer microstructure and higher hardness compared to the parts built in the interior region.
Electron Beam fusion:

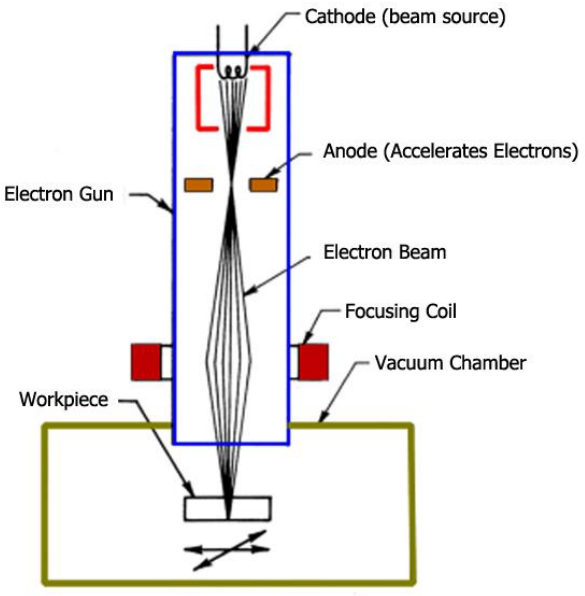

Figure 10: Electron Beam Melting Setup

Electron beam-powder bed fusion (EB-PBF) technique is a high-temperature AM process running in a relatively high vacuum chamber used to build high-temperature metallic parts. The EB-PBF as AM process is of interest due to its several advantages over conventional manufacturing processes, such as freedom to build intricate geometries, optimum material usage, elimination of expensive tooling, etc. Apart from the machine-related parameters such as scanning speed, beam current, focus offset, line offset.

It was found that the gap between the samples and height from the build plate affect the microstructural characteristics such as Nb-rich phase fraction and level of defects. However, the influence of the sample location due to a limited number of manufactured samples on the build plate did not show a clear trend. Similar to the effects of the gap between the samples and the height from the build plate on the microstructure, it is assumed that the part location shows similar behavior on the microstructure. There is a hypothesis that the innermost region (defined as “interior region”) of the build space is warmer, and the temperature radially decreases towards the outermost region (defined as “exterior region”). It can, therefore, be expected that parts built in the exterior region have a finer microstructure and higher hardness compared to the parts built in the interior region.

All the samples built in different locations (interior, middle, and exterior), elongated columnar grain structure perpendicular to the solidified layers along the build direction. Formation of the columnar structure was due to the sharp thermal gradient along the build direction during solidification. The observation of columnar grains is very common in EB-PBF built Alloy 718, in agreement with various literature, the effect of the location on the texture/orientation of the grains by the EBSD mapping samples of the exterior, middle, and interior samples, respectively. It is observed that for the sample located in the exterior region, the grains were slightly narrower due to the formation of stray grains between the columnar grains, which hindered the widening of the columnar grains. The formation of stray grains could be also due to the presence of more pores/lack-of-fusion defects which act as barriers and interrupt the columnar grain growth. The orientation of the grains was mainly sustained in the $< 001 >$ direction, and the disorientation was slightly higher in the exterior than the interior regions grain width was measured. It is found that the grains were slightly wider in the sample located in the interior of the build plate compared to the samples located in the exterior regions. The source of this slightly different microstructure is most likely related to the complex thermal history/thermal mass on the build plate during the EB-PBF process. In general, the solidified structure depends on the cooling rate, which is determined

by the processing parameters for each part built by EB-PBF.

The main types of the pores found in the samples manufactured in different locations were (a) spherical-shaped pores, which are assumed to be induced by the entrapped gas within the gas atomized powder particles and (b) solidification or shrinkage pores in form of strings of connected round pores. The shrinkage pores are typically found in inter dendritic regions and believed to be due to the lack of liquid to fill those regions during the last step of solidification. To study the influence of the sample's location on the amount of the defects, the content of the pores in the samples was measured. The results indicated that the level of pores was slightly greater in the samples located in the exterior regions of the build plate. The average values of the porosity content in the exterior and interior regions of the build plate were 0.40 ± 0.08 and 0.34 ± 0.06 area%, respectively. The variation in the level of pores measured in different samples could be attributed to the radial reduction of heat accumulation from the center to the edge of the build plate. This leads to a faster cooling rate in the exterior region, which is surrounded by more loose powder and subsequently results in formation of more shrinkage pores. The main reason for the creation of the shrinkage pores is a lower specific volume of the solidified material than that of the melted material. Contraction of the melted material during solidification occurs, and in the case of insufficient metal to fill the last region (inter dendritic area), the shrinkages pores form. At the higher cooling rate, primary dendrite arm spacing (PDAS) is finer, and there are larger inter dendritic regions. Subsequently, during solidification, the volume of the liquid flow in inter dendritic regions reduces due to contraction, leading to formation of a higher amount of the shrinkages pores.

5.1.2 Effect of Preheating Build Platform on Microstructure and Mechanical Properties of Additively Manufactured 316L Stainless Steel

This study aims to understand the effect of build platform preheating on the microstructural features and mechanical properties of 316L stainless steel (SS) fabricated via laser beam powder bed fusion (LB-PBF) process. Two sets of specimens were fabricated on a non-preheated build platform and the build platform preheated to 150 °C. Thermal simulations are carried out using ANSYS using additive manufacturing module to investigate the variation in thermal history experienced by the specimens in each condition. Microstructural features are analyzed via simulation, and the results are validated experimentally. In addition, the effect of preheating on the porosity size and distribution is evaluated using digital optical microscopy. Mechanical properties of specimens from each condition are further assessed and correlated to the variations in microstructure and defect size distributions.

Establishing process-structure-property-performance (PSPP) relationships for various material systems fabricated via additive manufacturing (AM) techniques has been becoming of particular interest for various industrial sectors. Although AM provides an opportunity to manufacture parts with complex geometries, the intricate thermal history experienced by the parts during fabrication leads to the formation of defects (i.e. pores, lack of fusion, surface roughness), producing anisotropic microstructure as well as inducing residual stress. As the most critical load-bearing parts are usually experiencing cyclic loading in service, it is essential to reduce defects and microstructure heterogeneity by controlling the thermal history.

Thermal history is controlled by the employed process parameters (i.e. laser power, scan speed, scan strategy, etc.), part size and geometry, build orientation, and the fabrication environment (due to shielding gas thermal properties and enclosure walls). These have been reported as the controlling parameters for reducing the defects and anisotropy in the microstructure and residual stress. Moreover, controlling thermal history may eliminate the need for post processing procedures (e.g. heat treatment, surface machining, hot isostatic pressing (HIP)), which expedites the adoption of AM for widespread industrial applications and reduces the cost of such procedures.

Accordingly, due to the complexity of changing process parameters such as laser power, scan speed, scan strategy, etc., fabricating parts by preheating the build platform can be a solution to

manufacture parts with more homogeneous microstructure and less residual stress. Austenitic stainless steel 316L is one of the most attractive materials in various industrial sectors. Moreover, its biocompatibility and corrosion resistance make this material suitable for medical applications such as bone implants. The goal of this study is to investigate the effects of build platform preheating on the microstructure and porosity level of LB-PBF 316L SS. Numerical simulations are carried out using ANSYS Additive Manufacturing module to calculate the variation in cooling rates. Numerical simulations are then validated by experimental observations of the melt pool dimensions and microstructural variation for different cooling rates. Eventually, the porosity size and distribution are evaluated for specimens fabricated with preheating the build plate and compared with the ones fabricated without preheating the build plate. Tensile deformation behavior is assessed for each condition and correlated to the microstructure and porosity size and distribution.

6.ABOUT THE DEPARTMENT

6.1 ADDITIVE MANUFACTURING

6.1.1 INTRODUCTION

- As per International committee F42 for Additive technologies, ASTM "Additive Manufacturing refers to a process by which digital 3D design data is used to build up a component in layers by depositing Materials".
- Additive manufacturing, also known as 3D printing, is a transformative approach to industrial production that enables the creation of lighter, stronger parts and systems. It is yet another technological advancement made possible by the transition from analog to digital processes.
- The seven different types of 3D printers

a. Fused deposition modeling (FDM)
b. Stereo lithography(SLA)
c. Digital Light Processing(DLP)
d. Selective Laser Sintering (SLS)
e. Selective laser melting (SLM)
f. Laminated object manufacturing (LOM)
g. Digital Beam Melting (EBM).

6.1.2 STEPS INVOLVED IN AM PROCESS

1. 3D model creation: Model is created using CAD software.
2. STL file creation: CAD Model is converted to STL file to slice it into digital layers.
3. STL file transfer: File is transferred to the printer using machine software.
4. Machine Set up: Required materials are loaded and setup with printing parameter.
5. Build: Printer builds the model by depositing material layer by layer.
6. Part Removal: Part is removed from the build platform and the support structures.
7. Post Processing: Such as cleaning, polishing and painting may be required.

6.1.3 POST PROCESSING OPERATIONS

- Machining
- Peening, Grinding

- Polishing, Surface treatment
- Heat treatment
- Hot isostatic pressing to eliminate residual porosities

6.1.4 ADVANTAGES

- Complexity is free: It actually costs less to print a complex part instead of a simple cube of the same size. The more complex (or, the less solid the object is), the faster and cheaper it can be made through additive manufacturing.
- Variety is free: If a part needs to be changed, the change can simply be made on the original CAD file, and the new product can be printed right away.
- No assembly required: Moving parts such as hinges and bicycle chains can be printed in metal directly into the product, which can significantly reduce the part numbers.
- Little lead time: Engineers can create a prototype with a 3-D printer immediately after finishing the part's stereo lithography (STL) file. As soon as the part has printed, engineers may then begin testing its properties instead of waiting weeks or months for a prototype or part to come in.
- Little-skill manufacturing: While complicated parts with specific parameters and high-tech applications ought to be left to the professionals, even children in elementary school have created their own figures using 3-D printing processes.
- Few constraints: Anything you can dream up and design in the CAD software, you can create with additive manufacturing.
- Less waste: Because only the material that is needed is used, there is very little (if any) material wasted.

7.MATERIALS EMPLOYED IN AM

7.1 Properties of Inconel 718

- **Inconel 718** is a nickel-chromium-molybdenum alloy designed to resist a wide range of severely corrosive environments, pitting and corrosion along with high yield and tensile strength. It is capable of withstanding surface temperature at about 1360 degree Celsius.
- When heated, **Inconel** forms a thick, stable, passivating oxide layer protecting the surface from further attack. This nickel steel alloy also displays exceptionally high yield, tensile, and creep-rupture properties at high temperature up to 1300ºF (705ºC.) The alloy has excellent weld ability. Its density is of 8.192 gram/cubic centimeter.
- **Applications** : Chemical processing, Aerospace, Liquid fuel rocket motor components, Pollution-control equipment, Nuclear reactors.

7.1.1 COMPOSITION of INCONEL 718

Element	Content in %
Nickel (Ni)	50.0 up to 55.0
Cobalt (Co)	1.00
Chromium (Cr)	17.0 up to 21.0
Molybdenum (Mo)	2.80 up to 3.30
Iron (Fe)	17.0
Silicon (Si)	0.35
Manganese (Mn)	0.35
Carbon (C)	0.08
Aluminum (Al)	0.60
Titanium (Ti)	0.90
Copper (Cu)	0.30
Phosphorous (P)	0.015
Boron (B)	0.006
Sulfur (S)	0.015
Niobium (Nb)+Tantalum (Ta)	4.75 up to 5.5

7.2 TITANIUM64

- **Ti-6Al-4V** also sometimes called **TC4** or Ti64, is an alpha-beta titanium alloy with a high strength-to-weight ratio and excellent corrosion resistance along with low modulus of elasticity, good weldability . This high-strength alloy can be used at cryogenic temperatures to about 800°F (427°C).

- Its **chemical composition** of almost 90% titanium, 6% aluminum, 4% vanadium, 0.25% (max) iron and 0.2% (max) oxygen. Its density is of 4.512gram/cubic centimeter.
- Ti-6Al-4V titanium alloy commonly exists in alpha, with hcp crystal structure, and beta, with bcc crystal structure, phases.
- Three common heat treatment processes are mill annealing, duplex annealing, and solution treating and aging.
- **Applications** : Additive Manufacturing, Parts and prototypes for racing and aerospace industry, Marine applications, Chemical industry, Gas turbines.

8.EOSINT M280

- The EOSINT **M 280** is an industrial 3D printer made by the German manufacturer EOS.
- The EOS EOSINT M 280 is based on the **DMLS** (Direct Metal Laser Sintering) 3D printing technology developed by EOS. This 3D printing technique uses a fiber laser to melt and fuse fine metal powder. Layer after layer the 3D object is built.
- This 3D printing method allows to create 3D printed products with complex geometries including elements such as freeform surfaces, deep slots and/or coolant ducts.

Figure 11: EOSM280

8.1 CONSTRUCTION:

The machine comprises a process chamber with recoating system, elevating system and platform

heating module, an optical system with laser, a process gas management system, a process computer with process control software, and a set of standard accessories. The machine components are integrated into a robust machine frame. During operation the process chamber is secured by interlock. Requirements of laser safety class 1 are met. When closed, the control cabinet's specifications correspond to IP 54. The system carries the CE designation.

8.2 SPECIFICATIONS

Optical system: The optical system creates and positions the laser beam to fuse (melt or otherwise solidify) the powder material. The laser emits a laser beam which is guided by an optical fiber, a beam expander optic, the scanner mirrors and a focusing objective. All optical surfaces have special coatings to guarantee effective beam guidance.

1. Laser

- Yb (Ytterbium) fiber laser
- Wavelength 1060 - 1100 nm
- Nominal power 195W

2. Scanner

- exposure area 250 mm x 250 mm
- exposure speed up to 7000 mm/s
- repeatability, scanner position < 11 µrad

3. Recoating and elevating system

The recoating system creates the layers of powder. It comprises a recoating element, a recoater arm and a linear drive, which moves the recoater arm in the horizontal direction. Different options are available for the recoating element. For titanium, aluminium and nickel alloys materials a high-speed steel (HSS) blade is recommended. For other materials a wear resistant ceramic blade is recommended. - Positioning speed 40 - 500 mm/s. The elevating system comprises dispenser, building and collector systems. The building system moves the platform carrier in the vertical direction. The part is built on a building platform which is mounted to the

platform carrier.

The building platform carrier has a three-point mounting and two motorized adjustment screws for simple and exact adjustment of the platform. In combination with a measurement tool which is mounted on the recoater arm, this allows a quick and easy alignment of the platform at the start of each job. It also includes reference positioning holes for precisely and reproducibly locating build platforms with corresponding positioning holes, by means of positioning pins. The building system has two parallel guide rails with backlash-free guides for highest positioning accuracy and long operating lifetime.

- Position repeatability $\leq \pm 0.005$ mm
- Maximum build height / z axis stroke 325 mm including building platform

4. Platform heating module

The platform heating module reduces temperature gradients between the building platform and the part to reduce internal stresses and ensure a good bonding of the first layers. It also removes any moisture from the powder and helps to maintain the part at a constant temperature during any interruptions in the building process to ensure maximum process reliability.

- operating temperature approx. 40 – 100 °C

5. Surface

´Surface' allows the production of parts or tools with fine, delicate geometries and highest requirements in terms of surface quality. Thinnest possible layer thickness is 20µm.

6. Performance

'Performance' offers high productivity with 40µm layer in 200W. Mechanical properties and density are identical with 'Surface' parameter set. Compared to 'Surface' parts 'Performance' parts production costs are reduced 40 – 50 %. Note: all these parameter sets produce fully-dense parts with comparable mechanical properties - see Material Data Sheets for further details.

7. Speed

This parameter set ´Speed'offers an optimal compromise between production speed and surface quality using 195W laser.

8. Building platforms

Parts are built on a building platform, which can either be integrated into the part (e.g. for tooling inserts) or separated from the parts after the building process. In the latter case the platform can normally be reused many times by re-machining the surface. Direct Base building platforms are 250 x 250 mm in size to fill the build area, and are attached to the carrier plate in the process chamber by four corner screws. They are available in various materials and specifications, as summarized in the table below:

Fig.: Building platform

Name	Material	Thickness	Features
DirectBase S22	1.1730 steel	22 mm	ground surface; 8 mm fixation holes
DirectBase S36	1.1730 steel	36 mm	ground surface; 8 mm fixation holes
DirectBase TS36P	1.2083 steel	36 mm	ground surface; 8 mm fixation holes; reference positioning holes; undercuts for Platform Handling option.
DirectBase Ti25	Ti6Al4V	25 mm	machined surface; 8 mm fixation holes
DirectBase AL30	Aluminium	30 mm	machined surface; 8 mm fixation holes

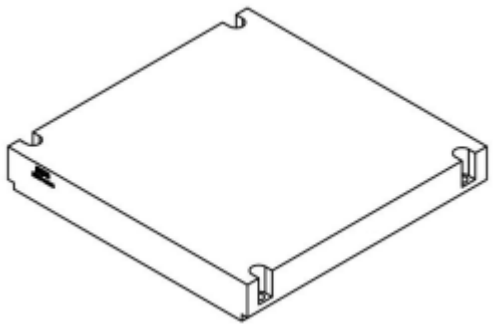

Figure 12: Build Platform

9. Precautions:

When using EOS Titanium materials, direct Base Ti25 platforms are recommended. When using EOS Aluminum AlSi10Mg, Direct Base AL30 platforms are recommended. When using EOS Maraging Steel MS1 material for heat treating parts whilst still on the platform, it is strongly recommended to use 1.2083 platform material (direct Base TS36P). When building heavy jobs, it is recommended to use platforms with undercuts in combination with the Platform Handling option (direct Base TS36P). See section 6.3.2 for details of the Platform Handling option. When building large or massive parts, it is recommended to use thicker platforms (e.g.36mm). When

building hybrid tools with EOS Maraging Steel MS1, we can only recommend 1.2709 steel as best suitable perform-alloy.

10. Data preparation Pre-processing of CAD data is necessary to create the SLI data which are required for the build process. The main requirement is the conversion of three-dimensional (3D) structures into a sequence of two-dimensional (2D) layers called "slices". Further requirements depend on the individual process chain from CAD design to the build process and may include repairing, cutting or scaling 3D structures. Applications which involve removing the built part from the building platform (typical Direct Part applications) require in addition the creation of supporting structures. The most commonly used conversion of CAD data is to the STL format, which approximates the part geometry by a net of triangles. Several software packages are able to work with part data in IGES, VDA-FS or other formats as well.

11. Materialize Magics RP

Magics RP is a software package for data pre-processing based on STL data. Materialise Magics is a versatile, industry-leading data preparation and STL editor software for Additive Manufacturing that allows you to convert files to STL, repair errors, edit your design and prepare your build platform. It is available for all current Windows operating systems and covers the needs of data pre-processing for EOSINT Systems:

- Visualization of parts in STL format
- Process compatible placement of parts
- Repairing and editing functions - quality assurance of STL files
- Reinforcements and supports (depending on part geometry and technology) using additional module SG or volume SG
- Import of IGES, VDA, CATIA and Unigraphics data using additional modules.

12. Argon gas:

In this mode the EOSINT M 280 system is set up to operate using an inert argon atmosphere. Reactive metals such as EOS Titanium, Inconel and Aluminium powders may only be processed using this operation mode. Most other materials such as nickel alloys and steels can also be

processed under argon atmosphere.

The following features are included in EOSINT M 280, many of which are required due to the higher safety requirements when working with argon gas and reactive metals:

- a connection to external bottle(s) or bottle battery of argon, as supplied by the user (see Installation Conditions)
- extended and redundant monitoring of the remaining oxygen content in several places, including process chamber, recirculating filter system and machine frame
- extended safety circuit including automatic interruption of the building process if a defined limit of oxygen content is exceeded When processing reactive metals such as EOS Titanium and Aluminium powders, the optional accessories wet separator (liquid-filled vacuum cleaner) and platform handling

9.PROCESS STEPS IN METAL ADDITIVE MANUFACTURING WORKFLOW

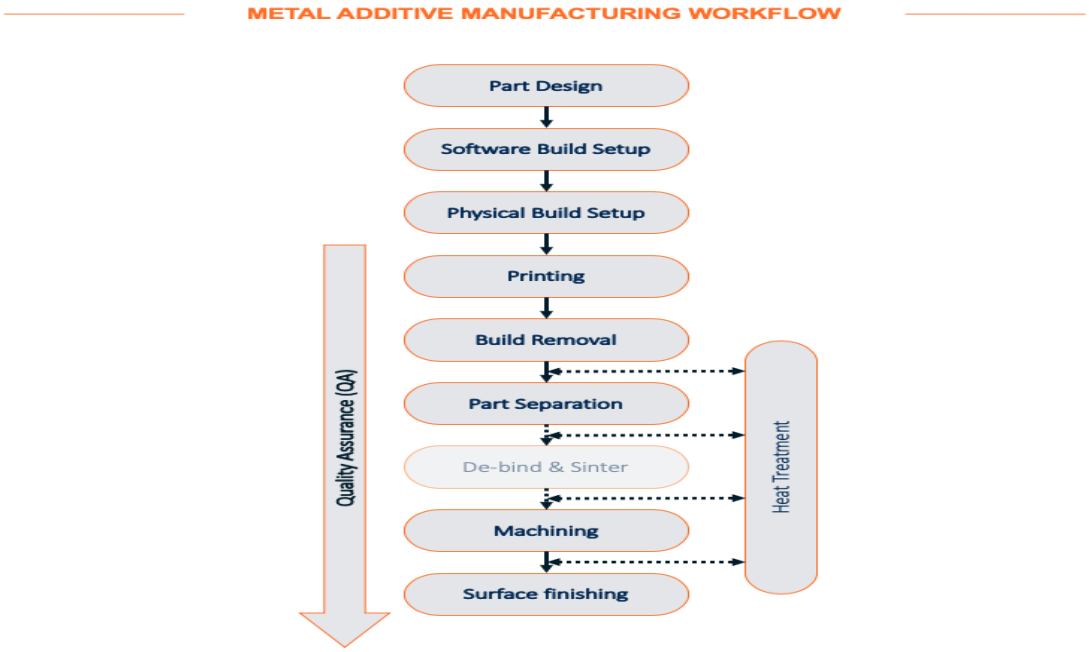

Figure 13: Additive Manufacturing Workflow.

A production manufacturing tool does not operate in isolation; it is tightly integrated into the upstream and downstream processes, and is only valuable when this integration is successful. Many publications about metal AM focus on the printing process, ignoring the important process steps that precede and follow. Implementing a successful Metal Additive Manufacturing (AM aka 3D Printing) production process requires more than installing and operating a printer. The entire AM workflow must be considered in evaluating, selecting, testing, and implementing a metal 3D printing solution.

Metal AM process steps depend on many factors including the technology, equipment, industry, and application. This post describes a general workflow which applies in most cases. We have structured this post by five key sections: Design, Pre-processing, Printing, Post-processing and Quality Assurance.

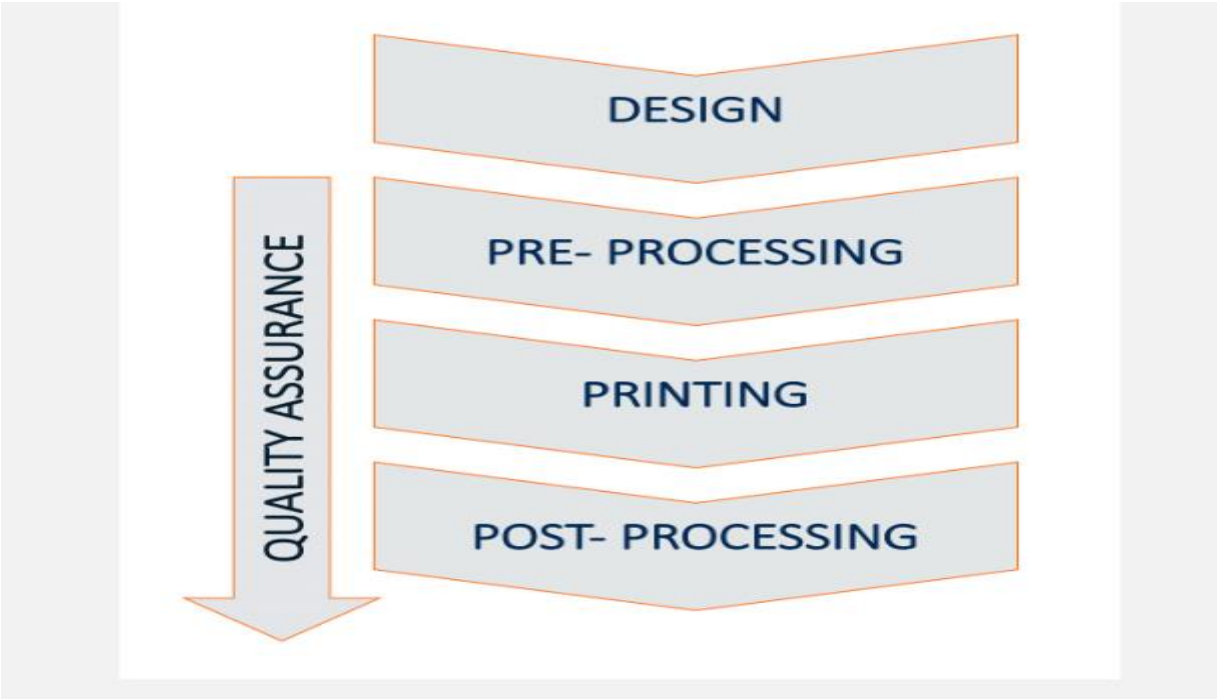

Figure 14: Steps In Additive manufacturing

9.1 Design

Design is the first step in the workflow. The challenges and opportunities in design for metal AM vary with whether a pre-existent part is chosen for printing or if a new part design is created.

For an existing part design, the objective is usually to select a production process that requires few modifications to the part. This reduces the costs of redesign and requalification. The business value for 3D printing in these cases will rely on time and production cost savings, rather than improved product performance. The time-to-value for metal AM is generally shorter if an existing part design is selected.

For a new, clean sheet design, design balances product function with manufacturability. Designing (or modifying) parts for 3D printing opens improved product performance as a potential driver of business value. Each metal AM process technology has its own design rules that limit part geometry and dictate the design of any structures needed to support the part during printing ("supports"). Engineers are increasingly turning to generative design and topology optimization to design for 3D printing, and new tools are coming to market for this task.

9.2 Pre Processing

Pre-processing encompasses the steps between design and printing. The first pre-processing step

is to convert a 3D CAD file into instructions the printer uses to build each layer of the part. These instructions are created by a "slicer", which slices the design file into layers of "voxels" (3D pixels) and generates a tool path for the printing process. The tool path incorporates both position information and print-process parameters (for example, power used to melt metal) for each voxel. There may be multiple parts in a single build, in which case organizing the parts efficiently on a build plate is an added step.

With some metal AM technologies, defining process parameters is a complex iterative process because the quality of metal printed and the accuracy of the print are highly sensitive to these parameters. In volume production, print parameters are often fixed and then maintained with ongoing machine calibration. In some technologies, process parameters are managed in real time with closed loop process control.

Once the software pre-processing and parameter development are complete, there is the physical setup of the machine. Physical setup includes:

- Loading and aligning the build plate or substrate,
- Preparing the printing chamber atmosphere (molten metal needs to be protected from oxygen), and
- Preparing and loading the feedstock for the printer. The complexity of these steps will depend on the feedstock type. As an example, metal powders require carefully handling due to their flammability, toxicity, and propensity to oxidize.

9.3 Printing

- Printing, while cool to watch, should actually be the process step that requires the least attention. Ideally, the 3D printer is able to run "lights out" with no operator monitoring or intervention. This is true today for more mature and stable processes and equipment.
- The printing step can take anywhere from minutes to many days, depending on the printing technology and size of the build. Most 3D printers heat the build plate or whole build envelope before printing. This can add considerable time which must be factored into cycle time calculations. Some processes require heat treatments for stress relief during the printing process which also adds time and cost to the printing step. Once a printing process is predictable enough that it doesn't need monitoring, the operator can spend print time on other tasks, improving overall productivity.

9.3.1 Principle of 3D processing

- DMLS follows the basic process sequence for most 3D printing technologies: model, slice, and print layer-by-layer. Once a 3D model is created and sliced with the appropriate software, the code needed for the printer to make the part is supplied to the printer, and the physical process can begin.

- To start, the DMLS printer hopper is filled with the desired metal powder. Printer heaters bring the powder to a temperature near the sintering range of the alloy. The printer uses an inert gas, which protects the heated powder and part as it is built.

- The build begins with dispensing a thin layer of metal powder onto the build platform. The laser then begins its path for this layer, selectively sintering the powder into a solid. The sequence of dispensing a layer and sintering continues until part completion.

- After the part is left to cool, the surrounding loose metal powder is removed from the printer. The last steps include support removal as well as any post-processing needed.
- DMLS parts can be treated like metal parts produced by conventional metal working for further processing. This may include machining, heat treatment, or surface finishing.

These process steps are shared with SLM, just with the laser's power turned up to "melt".

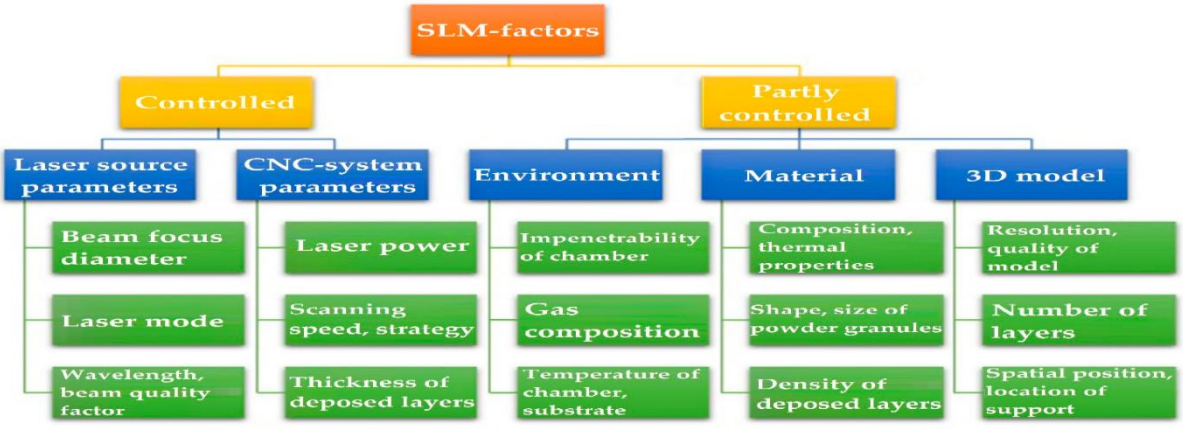

Figure 15: Input Parameters for the SLM process.

➢ Advantages

Direct metal printing: DMLS and SLM can produce metal parts directly. DMLS can be used with metal alloys or pure metals without affecting the properties of the material. Even mixtures of powders (e.g. aluminum and nylon) can be successfully printed.

Variety of materials: Between DMLS and SLM, a wide range of metal and metal alloy powders are available, including steels, stainless steels, aluminum, titanium, nickel alloys, cobalt chrome, and precious metals.

Strong, functional parts: The properties of a finished part are comparable to a part cast in the same material. Strong, functional metal parts are produced by the DMLS process. SLM can produce a stronger part by melting the metal. Final parts have good mechanical properties in all directions. (Some 3D printing methods — e.g. FDM — tend to be weak in at least one direction.) Recyclable material: Metal powder that is not sintered or melted is reusable.

➢ Limitations

High pricing: DMLS and SLM have the highest price points of 3D printing processes; the machines and materials are expensive, and the process is slow.

Porous parts: Finished DMLS parts are porous relative to a melted metal part. Porosity can be controlled but not eliminated in the process or during post-processing.

Small parts: Most DMLS printers have relatively small build volumes.

9.4 Post Processing

Post-processing steps vary widely between various AM processes, equipment, applications, etc. The steps have to be designed carefully to meet all the part requirements (e.g. accuracy, surface roughness, strength, etc.) and this is another area where iteration and testing are typically needed for program validation. Most of the key steps are outlined below.Post-processing steps vary widely between various AM processes, equipment, applications, etc.

The steps have to be designed carefully to meet all the part requirements (e.g. accuracy, surface roughness, strength, etc.) and this is another area where iteration and testing are typically needed for program validation.Steps involved are as follows:

9.4.1 Build Removal

- Removing excess material from the build inside the printer (e.g. in powder bed processes)
- Removing the build from the printer
- Inspection for accuracy, potential delamination, surface quality, support attachments, etc.

9.4.2 Part Separation

- Removing parts from the build plate, using EDM, band saw or machining
- Removing parts from each-other if attached for nesting purposes
- Removing supports from individual parts, often requiring clippers, EDM, band saw or machining (support removal can also be completed in secondary machining steps)

a) **De-binding and Sintering (only for binder processes)**

- Soaking parts in solution for up to a couple days to remove binding materials from the metal
- Sintering highly porous parts from previous step to reduce porosity

b) **Machining**

- Machining to remove remaining supports, smooth surfaces, add critical features, and hit critical tolerances
- Custom fixtures may need to be created to hold printed parts for secondary operations. If the part geometry is complex or organic, these fixtures can become resource intensive to design and manufacture

9.4.3 Surface Finishing

- Polishing surfaces where surface roughness requirements were not achievable from machining
- Tumbling or Shot peening to smooth and/or work harden surfaces, or mitigate issues with loose powder on unfinished surfaces.

a)Micro shot-peening is a post-processing method which enables the surface quality to be significantly improved very quickly and easily, both for direct use and as a basis for further polishing. It is strongly recommended for all materials. Depending on the application, the

following packages are recommended. Detailed recommendations for certain applications are included in the Application Notes "Surface finishing of DMLS parts". For applications which demand a high metallurgical purity, for example medical implants, it is necessary to carefully consider which peening media to use and how to handle the parts.

b)Sandblasting is also known as **abrasive blasting**. Basically, it is the operation of forcibly propelling a stream of **abrasive** material against a surface. The **sandblasting** operation is done under high pressure to smooth a rough surface, roughen a smooth/Shape the surface to remove its contaminants.

c)Abrasive blasting uses various materials to strip imperfections, paint, rust and other contaminants from a surface. It's an important step in surface coating preparation, as it cleans a substrate and creates a surface that will hold a protective coating. Silica Sandblasting was a commonly used method of removing impurities from surfaces; this is because sand particles are almost the same size and the edges of the particles are sharp, hence making this type of grit efficient in abrasive blasting.

9.4.4 Heat Treatment (HT): Heat Treatment is defined as a controlled operation that involves the heating and cooling of a metal or alloy in the solid state for the purpose of obtaining certain desirable shape of metal. The process of converting the solid metal into desired shape by heating is known as heat treatment process.

The purpose of heat treatment are as follows:

- Improve ductility and toughness
- Harden and strengthen metals
- Improve machinability
- Change grain size
- Homogenize the structure to remove coring

The stages involved in heat treatment:

- Heat the metal slowly to ensure uniform temperature.
- Soak/hold the metal at a given temperature and time.
- Cool the metal to room temperature.

Types of heat treatment:

1.Annealing: Annealing is a heat treatment process which alters the microstructure of a material to change its mechanical properties. Typically, in steels, annealing is used to reduce hardness, increase ductility and help eliminate internal stresses.

Two heat treatments are generally utilized for INCONEL alloy 718:

•Solution anneal at 1700-1850°F followed by rapid cooling, usually in water, plus precipitation hardening at 1325°F for 8 hours, furnace cool to 1150°F, hold at 1150°F for a total aging time of 18 hours, followed by air cooling.

•Solution anneal at 1900-1950°F followed by rapid cooling, usually in water, plus precipitation hardening at 1400°F for 10 hours, furnace cool to 1200°F, hold at 1200°F for a total aging time of 20 hours, followed by air cooling.

If the material is to be machined, formed, or welded, it typically is purchased in the mill annealed or stress relieved condition. The material is then fabricated in its most malleable condition. After fabrication, it can be heat treated as required per the applicable specification

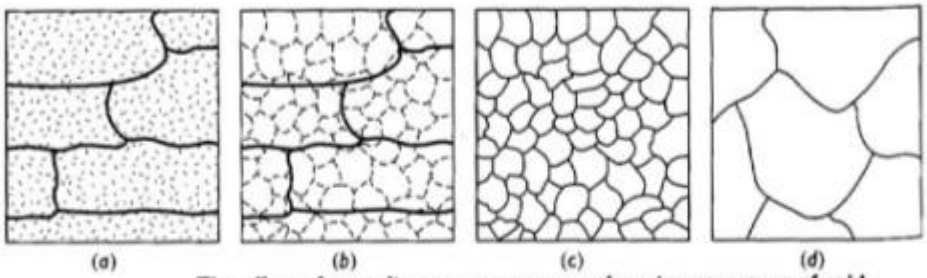

The effect of annealing temperature on the microstructure of cold-worked metals: (a) cold worked, (b) after recovery, (c) after recrystallization, and (d) after grain growth.

Figure 16: Effect of annealing on Microstructure.

Recovery: softening through removal of dislocations and internal stresses
Recrystallization: nucleation of new strain-free grain.
Grain growth: coarsening of grains.

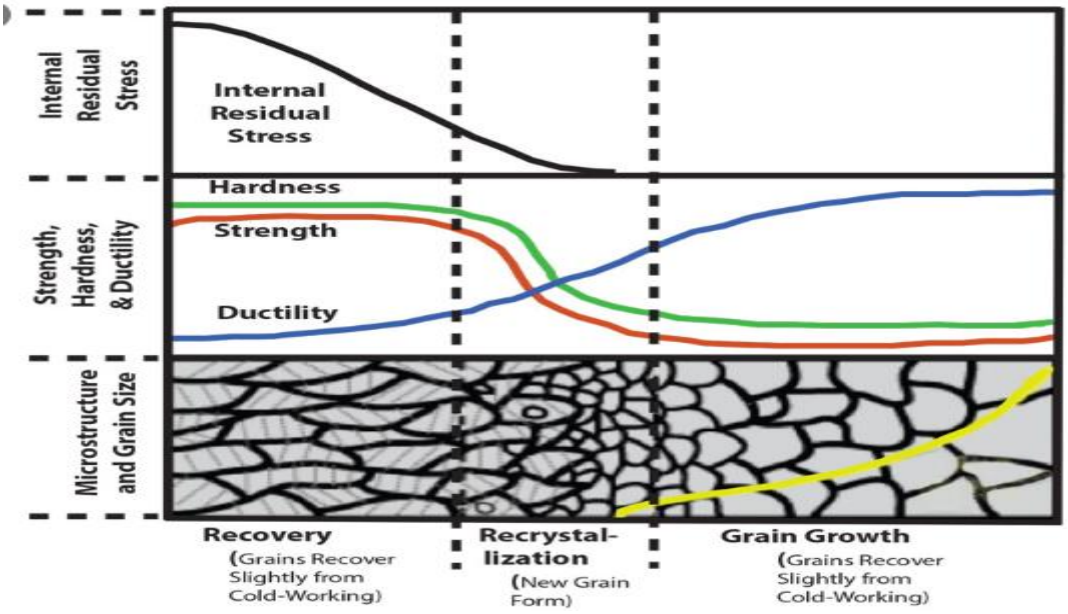

Figure 17: Effect of Microstructure on Mechanical properties.

2.Normalizing: Normalizing process is a heat treatment process for making material softer but does not produce the uniform material properties as produced with an annealing process. The most common reason for the normalizing process is to adjust mechanical properties to suit the service conditions. The usual normalizing temperature ranges from 815°C to 980°C (1500°F to 1800°F), depending on the steel involved.

3. Hardening: Hardening is a metallurgical metalworking process used to increase the hardness of a metal. The hardness of a metal is directly proportional to the uniaxial yield stress at the location of the imposed strain. A harder metal will have a higher resistance to plastic deformation than a less hard metal.

a)Age hardening, also called **precipitation hardening**, is a secondary **heat treatment** technique used to increase the strength of some **alloys**. The first step of aging is to fully anneal the material, then a second lower temperature **heat treatment** is performed to **age harden** the material.

Hot Isostatic Pressing (HIP) often used by powder processes after part separation to decrease porosity and further relieve stresses .Furnace Sintering, required for powder binder processes after binder removal. It can result in a lot of shrinkage and drift in geometry. This must be compensated for upstream at the design stage and managed closely with QA.

HT before machining to temper the material and reduce hardness (due to rapid cooling in most metal printing processes, the material can be in a highly hardened state that is difficult to machine)

HT after machining to achieve final hardness requirements and desired metallurgy phases and grain structure.

b)Double age hardening:

Refined grain size and microstructure of the core of the part, grown during long duration at high temperature

Avoids surplus/retained austenite content in the case depth

Reduces or limits the distortion level of parts with complex shapes

Adjusts more precisely the hardness of the core and the case

4.Case-hardening or **surface hardening** is the process of hardening the surface of a metal object while allowing the metal deeper underneath to remain soft, thus forming a thin layer of harder metal (called the "case") at the surface.

Case-hardened steel is formed by diffusing carbon (carburization), nitrogen (nitriding) and/or boron (boriding) into the outer layer of the steel at high temperature, and then heat treating the surface layer to the desired hardness.

10. Description of INCO-718

10.1 Gas Atomization of INCO-718

Gas atomization of liquid melts several principle atomisation mechanisms and devices exist for disintegration of molten metals. An overview on molten metal atomisation techniques and devices is given e.g. by (Lawley, 1992; Bauckhage, 1992; Yule & Dunkley, 1994, and Nasr et al., 2002). In the area of metal powder production by atomisation of molten metals typically twin-fluid atomisation by means of inert gases is used. Main reasons for using this specific atomisation technique are: - the possibility of high throughputs and disintegration of high mass flow rates - the greater amount of heat transfer between gas and particles for rapid partially cooling the particles - the direct delivery of kinetic energy to accelerate the particles towards the substrate/deposit for compaction - the minimization of oxidation risks of the atomized materials within the spray process by use of inert gases. Hybrid Gas Atomization for Powder Production 101 A common characteristic of the used variations of twin-fluid atomizers for molten metal atomisation is the vertical exit of the melt jet from the tundish via the (in most cases cylindrical) melt nozzle in the direction of gravity. Also in most cases the central melt jet stream is surrounded by a gas flow from a single (slit) jet configuration or a set of discrete gas jets, which are flowing in parallel direction to the melt flow or within an inclination angle of attack towards the melt stream. The coaxial atomizer gas usually exits the atomizer at high pressures with high kinetic energy. Two main configurations and types of twin-fluid atomizers need to be distinguished within molten metal atomisation. The first kind is called the confined or close-coupled atomizer and the second kind is called the free-fall atomizer. Both concepts are shown.

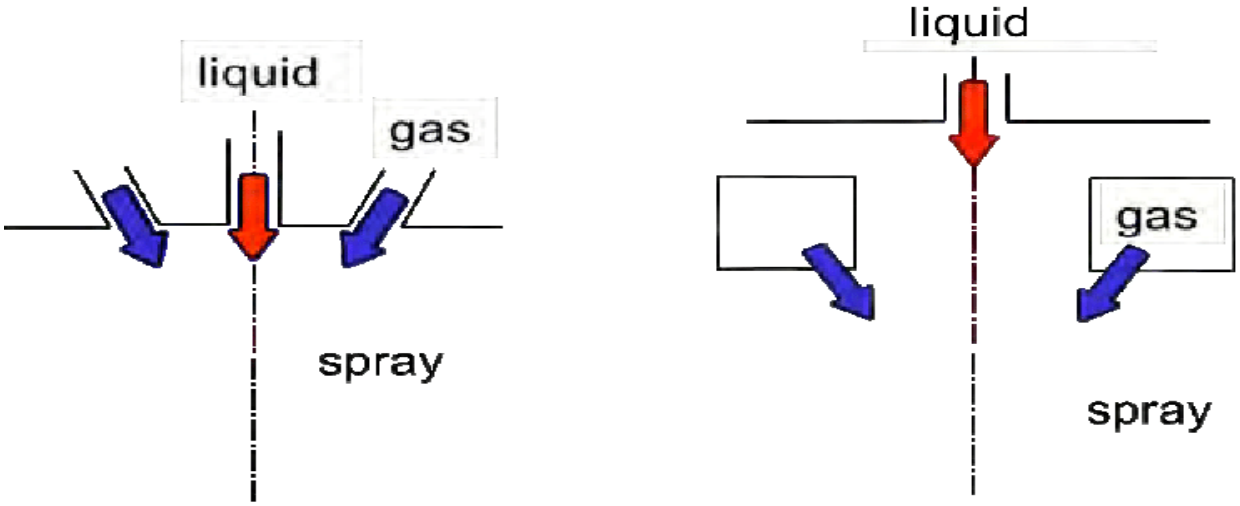

Figure 18: Gas atomisation OF INCO 718

The gas flow in the close-coupled atomizer immediately covers the exiting melt jet. Within the confined atomizer the distance between gas exit and melt stream is much smaller than in the free-fall arrangement, where the melt jet moves a certain distance in the direction of gravity before the gas flow impinges onto the central melt jet. The close-coupled configuration generally tends to yield higher atomisation efficiencies (in terms of smaller particles at identical energy consumption) due to the lower distance between the gas and melt exits. But the confined atomizer type is more susceptible for freezing problems of the melt at the nozzle tip. This effect is due to the extensive cooling of the melt by the expanding gas flow, which exits in the close-coupled type nearby to the melt stream. During isentropic gas expansion the atomisation gas temperature is lowered (sometimes well below 0°C). Because of the close spatial coupling between gas and melt flow fields, this contributes to a rapid cooling of the melt at the tip of the melt nozzle. The freezing problem is relevant especially for spray forming applications. In this process, in all technical applications a discontinuous batch operation is performed (e.g. due to the batch wise melt preparation or the limited preform extend to be spray formed). The operational times of spray forming processes are ranging from several minutes up to approximately one hour. The thermal related freezing problem is most important in the initial phase of the process directly when the melt stream exits the nozzle for the first time. At that point the nozzle tip is still cool and needs to be heated first e.g. by the hot melt flow. This heating process lasts a certain time. Therefore, thermal related freezing problems are often to be observed in the first few seconds of a melt atomization process. 102 Powder Metallurgy In addition to the thermal related freezing problem within the melt nozzle, also chemical or metallurgical related problems in melt delivery systems are found frequently. Not all of these problems are solved yet in melt atomisation applications. A range of problems arises from the possible change of material composition of the melt, or that of the tundish or nozzle material, due to possible melt/tundish reactions or melt segregational effects from diffusion. This reaction process kinetics is somewhat slower than the thermal freezing process kinetics mentioned before and may contribute to operational problems at a later temporal state of process operation.

10.2 Powder Characteristics of INCO 718

a) Particle size:

A HORIBA LA-960 laser particle size analyzer was used in accordance with the ISO 13320-1

standard to quantify the particle size, PSD, and particle fraction at specific particle sizes using the laser-scattering technique. A small quantity of each IN718 powder sample, with a refractive index of 1.958, was poured into deionized water with a refractive index of 1.333. The powders were mechanically and ultrasonically stirred, circulated, and degassed before measurement. Five consecutive readings were taken in the automatic mode and five measurements were carried out in the manual mode to confirm the consistency of the results. The results are shown in fig below. Table 2 PSD and Hall flow rate of virgin and recycled IN718 powders. Material D10 (μm) D50 (μm) D90 (μm) Hall flow rate (s·(50 g)–1) Virgin 21.37 ± 0.43 31.24 ± 0.97 49.52 ± 0.76 28.35 ± 0.32 Recycled 21.92 ± 0.54 32.35 ± 0.78 50.71 ± 0.85 29.47 ± 0.42 ”D10”, “D50”, and “D90” mean the particle sizes at 10 vol%, 50 vol%, and 90 vol%, respectively.

b)Flow ability:

Measurement is conducted using a Hall flowmeter The Hall flow rate of these powders was measured in accordance with the ASTM B213 standard test method. A 50 g mass of each powder was weighed to an accuracy of 0.0001 g and gently poured into the Hall flowmeter funnel. The discharge orifice at the bottom of the funnel was then unlocked to let the powder flow naturally. A timing device was started simultaneously to record the flow duration.

c)Chemical composition of virgin and recycled IN718 powders. Material Ni Ti Cr Mo Nb Fe C Mn Si Al Co Cu Virgin (wt %) 52.35 0.85 20.12 3.04 5.10 Balance 0.013 0.09 0.08 0.60 0.16 0.012 Recycled (wt%) 52.32 0.83 20.15 2.96 5.05 Balance 0.019 0.08 0.08 0.55 0.15 0.011

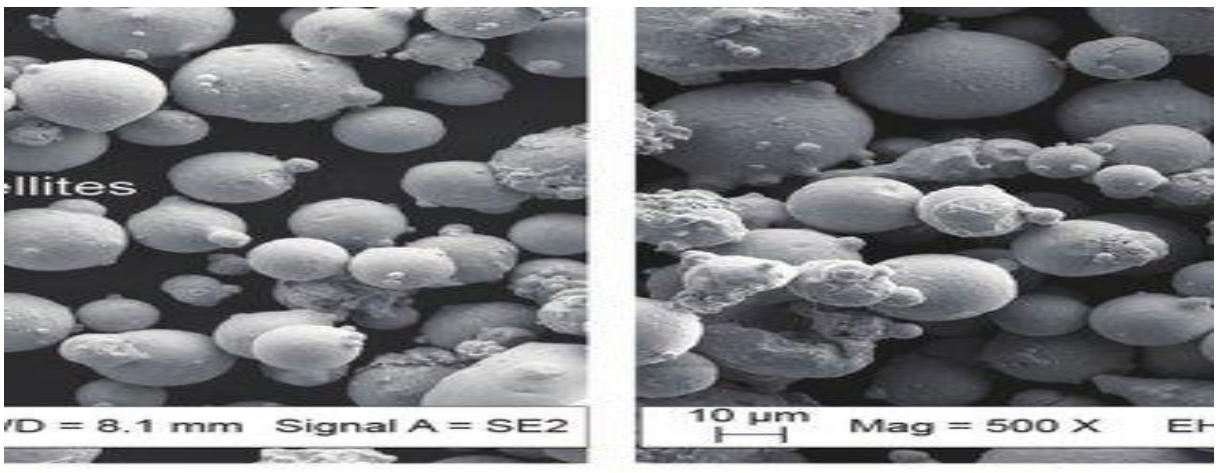

Figure 19: Microstructure of INCO 718

d)The surface roughness measured along the sintered surface of the sintered Inconel-625 in inert atmosphere. It is evident from the figure that the surface roughness increases with the

increase in the laser scan speed. It is also clear from the figure that Inconel-625 sintered at a laser scan speed of 2.5 mm/s are smooth compared to those sintered at 10 mm/s. The surface topographies taken from the confocal microscope shown below also confirms the presence of the variable sharp peaks for the higher scan speed and moderate peaks for lower scan speed. The variation of the surface finish with laser scan speed can be explained in terms of the laser energy density. When the scan speed is low, the laser energy density is high, as laser density is inversely proportional to the laser scan speed. Literature also confirms that the surface roughness is a function of laser power density and line spacing. The powders will be fully melted at lower scan speed, resulting in reduced melt viscosity, balling effect and increased melt cylinder diameter, leading to better connectivity and reduction in the inter pore size.

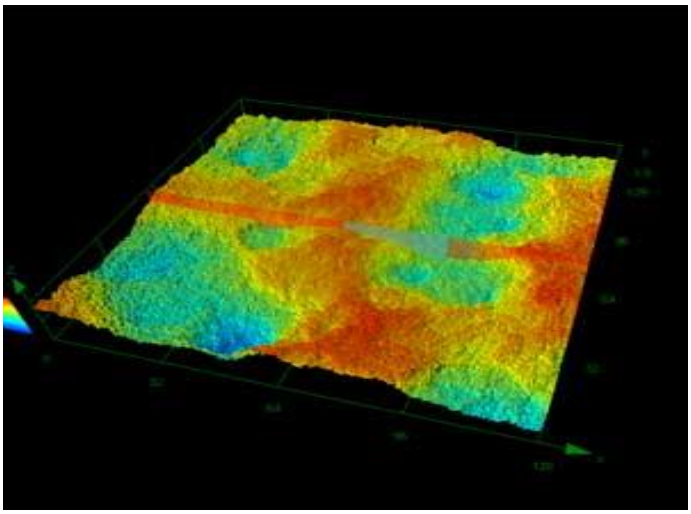

Figure 20: Surface Topographies taken by a confocal microscope.

10.3 Porosity:

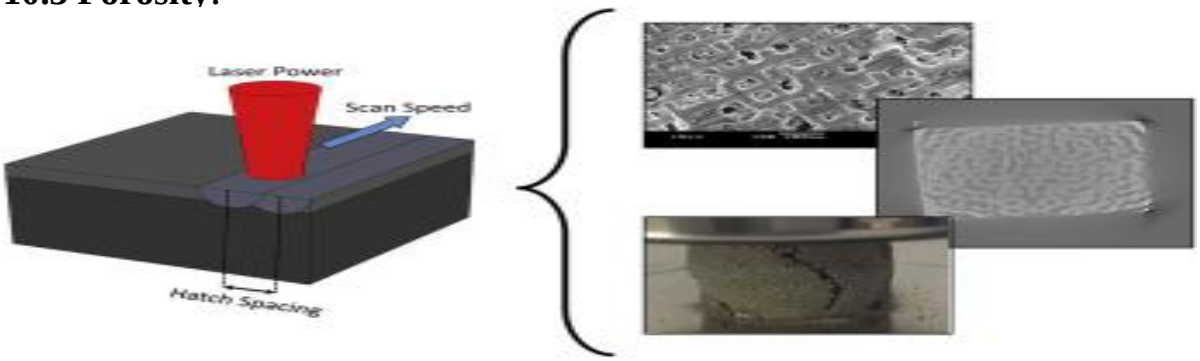

Figure 21: Porosities present SLM manufactured parts.

The melt pool characteristics in terms of size and shape and the porosity development in laser powder bed fusion–processed Inconel 718 were investigated to determine how laser power and scan speed influence the porosity in the microstructure. The melt pool characteristics developed with both single-track and multilayer bulk laser deposition were evaluated. It was found that the melt pool characteristic is critical for the porosity development. It is shown that the porosity fraction and pore shape change depending on the melt pool size and shape. This result is explained based on the local energy density of a laser during the process. High-density (> 99%) Inconel 718 samples were achieved over a wide range of laser energy densities (J/mm2). A careful assessment shows that the laser power and scan speed affect differently in developing the pores in the samples. The porosity decreased rapidly with the increase in laser power while it varied linearly with the scan speed. A proper combination, however, led to fully dense samples. The study reveals an optimum condition in terms of laser power and scan speed that can be adopted to fabricate high-density Inconel 718 parts using laser powder bed fusion–based additive manufacturing process.

10.4 Grain boundary:

Inconel 718 fabricated by selective laser melting (SLM) was used to investigate the evolution of grain boundary (GB) network structures from as-SLM to heat-treated (HT) samples. Using electron backscatter diffraction (EBSD) data and percolation theory based cluster analysis, GB character distribution and GB network topological metrics were computed at different build locations and directions. The microstructures of the as-SLM samples reveal large spatial heterogeneity in grain morphology and are dominated by general GBs, which form one connected cluster spanning across the whole GB network. Heat-treatment homogenizes the microstructure and leads to the formation of annealing twins as a result of recrystallization, which dramatically increases the number of special boundaries (mainly twin and twin-related boundaries with ~ 60% in boundary length fraction). However, these special boundaries have not yet fully connected/merged to form a percolated path throughout the GB network. The triple junction distributions of the HT sample are dominated by J_1-type that consists of one special and two general boundaries, further confirming the interweaving GB network made of the general and special boundary clusters. In addition, the implication of applying GB engineering to the SLMed parts is discussed based on the comparison of GB network structures between the SLMed alloys

and the conventionally GB engineered metals and alloys.

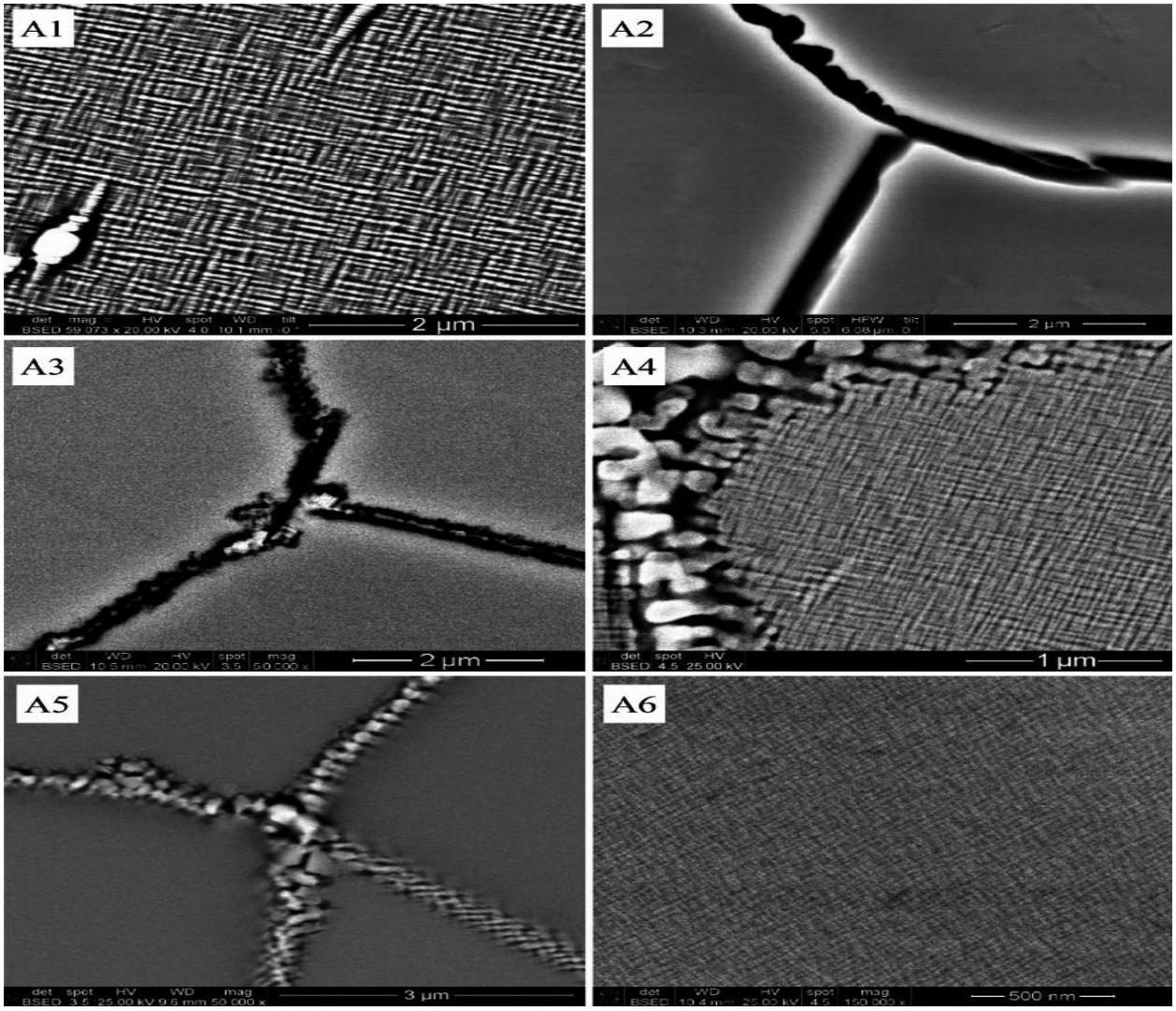

Figure 22: Fine microstructure of grain interior and grain boundaries of the A1–A6 HEAs.

11. PART QUALITY

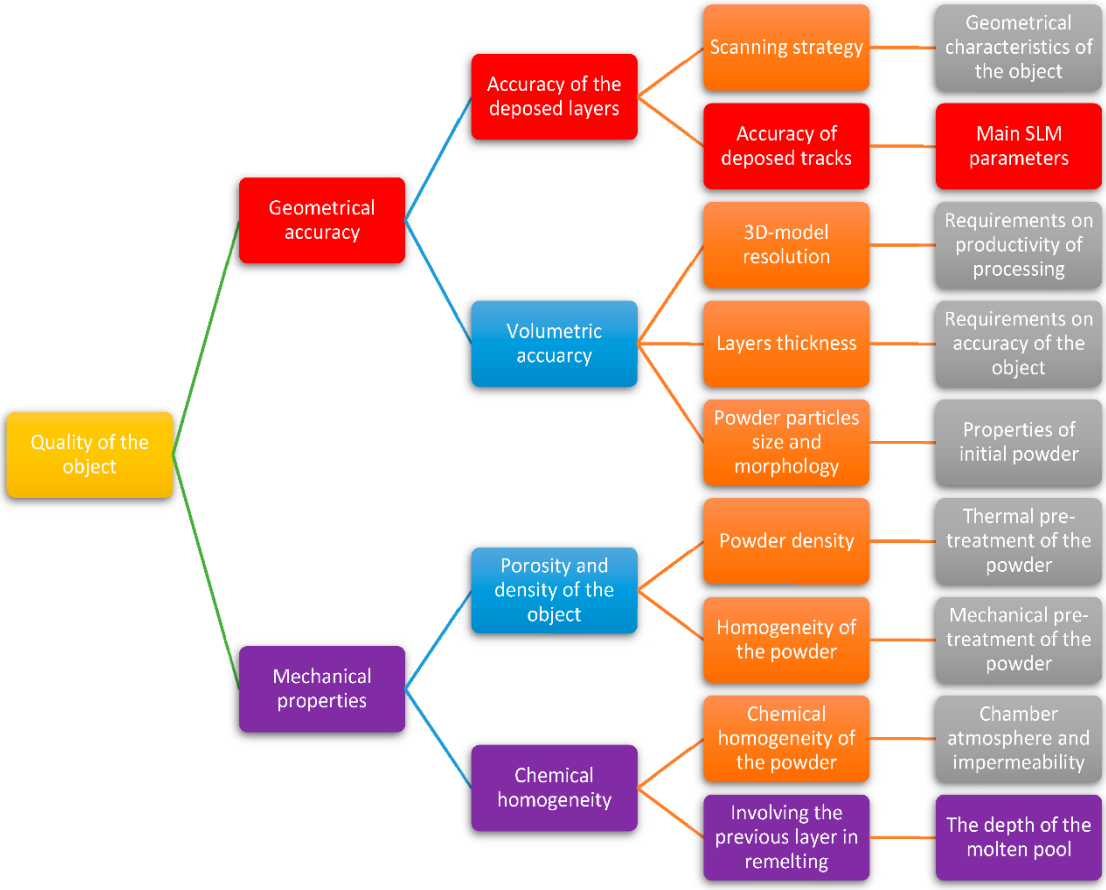

Figure 23: Part quality determining Parameters.

12. RESIDUAL STRESS

12.1 INTRODUCTION

Residual Stress is the stress that remains in a material or body after manufacture and processing in the absence of external forces.

Origins of residual stress

- Mechanical
- Thermal
- Chemical

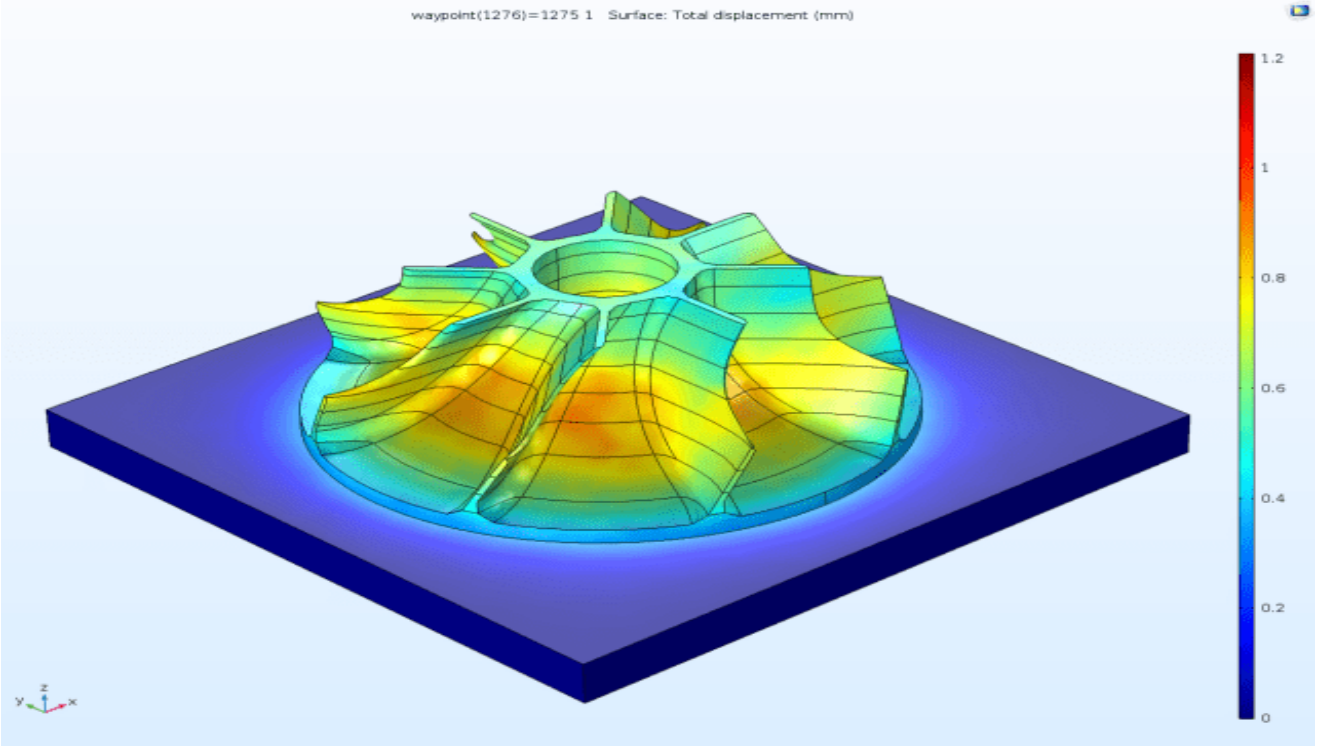

Figure 24: Residual Stress distribution

12.2 COMPONENTS USED TO MESURE RESIDUAL STRESS

12.2.1 XRD Characteristics:

X-rays were discovered by Wilhelm Roentgen who called them x - rays because the nature at first was unknown so, x-rays are also called Roentgen rays. X-ray diffraction in crystals was

discovered by Max von Laue. The wavelength range is 0.01 to about 10 nm. X-rays are short wave length electromagnetic radiations produced by the deceleration of high energy electrons or by electronic transitions of electrons in the inner orbital of atoms .The penetrating power of x-rays depends on energy also, there are two types of x-rays. i) Hard x-rays: which have high frequency and have more energy. ii) Soft x-rays: which have less penetrating and have low energy.

X-ray Diffraction (XRD) is a non-contact and non-destructive technique used to understand the crystalline phases, different polymeric forms and the structural properties of the materials ← X – ray diffraction "Every crystalline substance gives a pattern; the same substance always gives the same pattern; and in a mixture of substances each produces its pattern independently of the others" -Words by Wilhelm Rontgen at the time of Nobel speech. ← The X-ray diffraction pattern of a pure substance is, therefore, like a fingerprint of the substance. It is based on the scattering of x-rays by crystals. ← Definition the atomic planes of a crystal cause an incident beam of X- rays to interfere with one another as they leave the crystal. The phenomenon is called X- ray diffraction.

- **Principle of X ray diffraction**

X-ray diffraction is based on constructive interference of monochromatic x-rays and a crystalline sample. These x-rays are generated by a cathode ray tube, filtered to produce monochromatic radiation, collimated to concentrate and directed towards the sample. The interaction of incident rays with the sample produces constructive interference when conditions satisfy Bragg's law.

Braggs law= λ=2 sin□ d/n

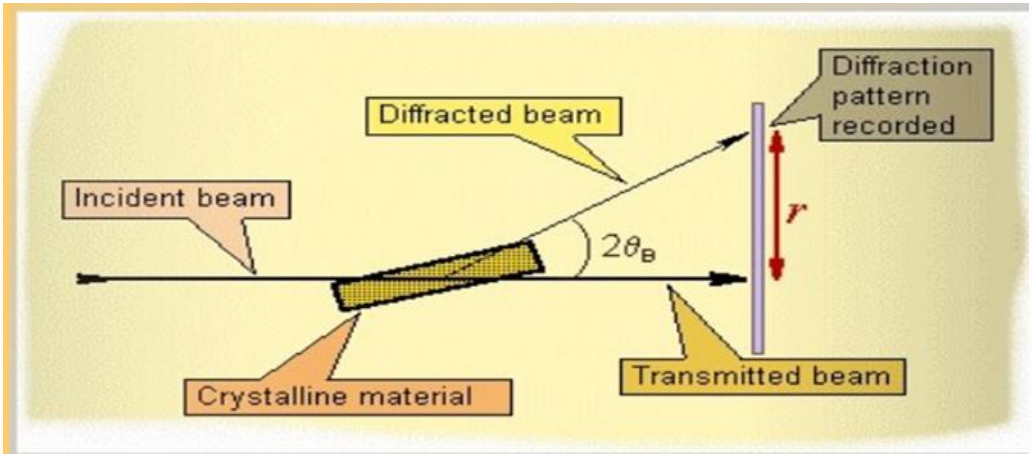

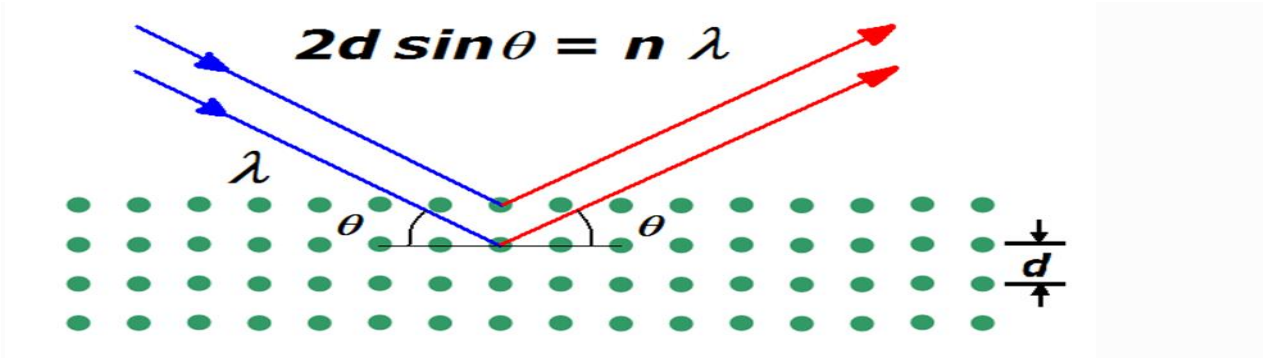

Figure 26: Braggs Law

Figure 25: XSTRESS 3000:

Key Features

- Replaceable, to provide 1, 2, 3, 4, and 5 millimeter Control of residual stresses
- Retained austenite measurements
- Accuracy at the laboratory
- No parts cutting
- Measurements in hard-to-reach areas
- Works as dial indicator for etching depth measurements
- Flexibility in field applications
- Custom inspection stations
- Measurement services spot sizes. Special collimators available as an optional extra.

- X ray Tube
- Miniature, 30 kV/6.6–10 mA/200–300 W;
- Cr, Cu, Co, Fe, V, Ti, Mn. Cr-tube provided as a standard. Tube can be replaced in less than ten minutes without special tools

Goniometer:

- Xstress 3000 goniometer type G3 mounted on a tripod with magnetic anchoring as standard
- X-inclination: Programmable, max. –58° to+58°
- χ-oscillation: Freely programmable
- Distance between goniometer and the measurement point automatically adjusted to ± 0.001 mm accuracy.
- Detectors:
- Dual position sensitive MOS Linear Image
- Sensors in symmetrically χ (side inclination) geometry
- Angular resolution: 0.014°–0.057°/pixel 2θ-angle is instantly adjustable by manually sliding the detectors to the desired angular position along the arc-shaped detector holder

12.2.2 3D White Light and 3D Laser Scanners

3D white light scanners are usually tripod mounted. Scan data is obtained shot by shot, as a grid of light is projected and laid over the component being scanned. As a scan is completed the grid is modified, and the scanner determines the 3D coordinates by calculating the returned patterns.

3D laser scanners are usually handheld or tripod mounted, and scan data is obtained as a laser stripe sweeps over a component or entire area. The handheld type is typically attached to an arm, which provide a constant readout of where the scanner is at any time.

A white light scanner (WLS) is a device for performing surface height measurements of an object using coherence scanning interferometry (CSI) with spectrally-broadband, "white light" illumination. Different configurations of scanning interferometer may be used to measure macroscopic objects with surface profiles measuring in the centimeter range, to microscopic objects with surface profiles measuring in the micrometer range. For large-scale non-interferometric measurement systems, see structured-light 3D scanner.

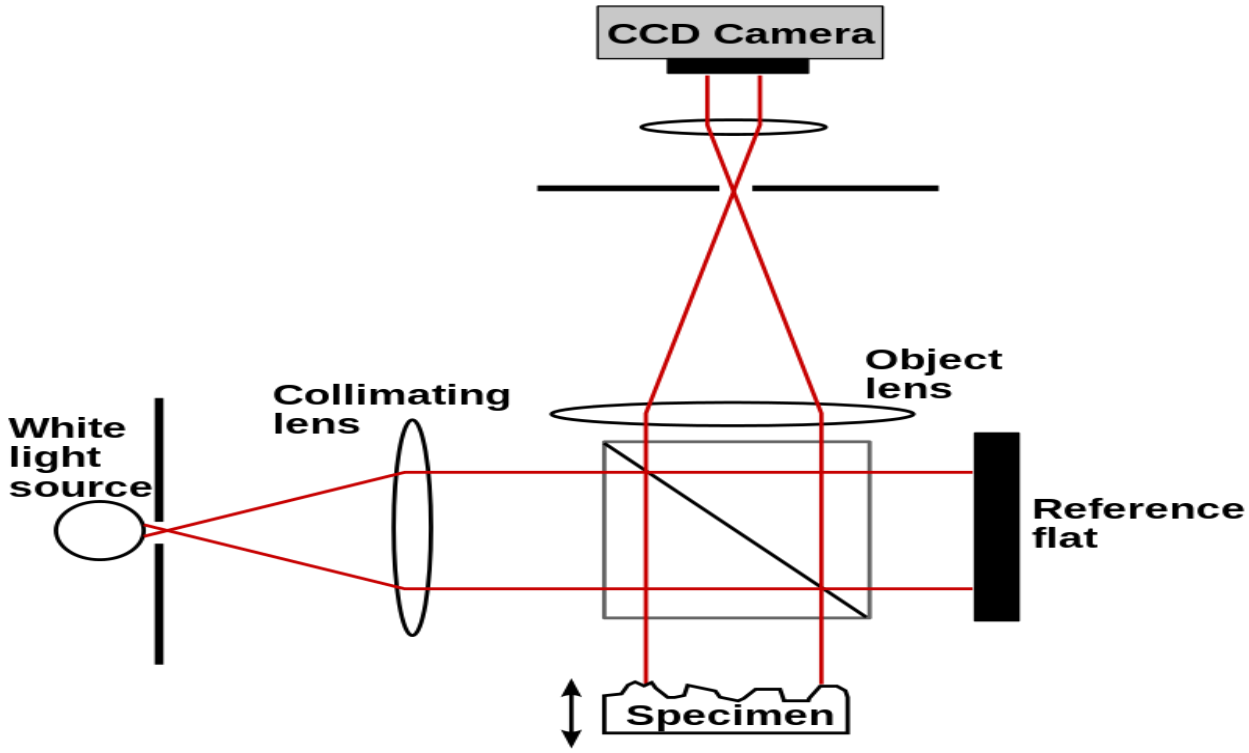

Figure 27: Basic Components of white Light Scanners.

➢ Description:

Vertical scanning interferometry is an example of low-coherence interferometry, which exploits the low coherence of white light. Interference will only be achieved when the path length delays of the interferometer are matched within the coherence time of the light source. VSI monitors the fringe contrast rather than the shape of the fringes.

Above fig illustrates a Twyman–Green interferometer set up for white light scanning of a macroscopic object. Light from the test specimen is mixed with light reflected from the reference mirror to form an interference pattern. Fringes appear in the CCD image only where the optical path lengths differ by less than half the coherence length of the light source, which is generally on the order of micrometers. The interference signal (correlogram) is recorded and analyzed as either the specimen or reference mirror is scanned. The focus position of any particular point on the surface of the specimen corresponds to the point of maximum fringe contrast (i.e. where the modulation of the correlogram is greatest).

Other forms of interferometer used with white light include the Michelson interferometer (for low magnification objectives, where the reference mirror in a Mirau objective would interrupt too much of the aperture) and the Linnik interferometer (for high magnification objectives with limited working distance). The objective (or alternatively, the sample) is moved vertically over the full height range of the sample, and the position of maximum fringe contrast is found for each pixel.

The chief benefit of low-coherence interferometry is that systems can be designed that do not suffer from the 2 pi ambiguity of coherent interferometry, and as seen in Fig. 27, which scans a 180 μm × 140 μm × 10 μm volume, it is well suited to profiling steps and rough surfaces. The axial resolution of the system is determined by the coherence length of the light source and is typically in the micrometer range. Industrial applications include in-process surface metrology, roughness measurement, 3D surface metrology in hard-to-reach spaces and in hostile environments, profilometry of surfaces with high aspect ratio features (grooves, channels, holes), and film thickness measurement (semi-conductor and optical industries, etc.)

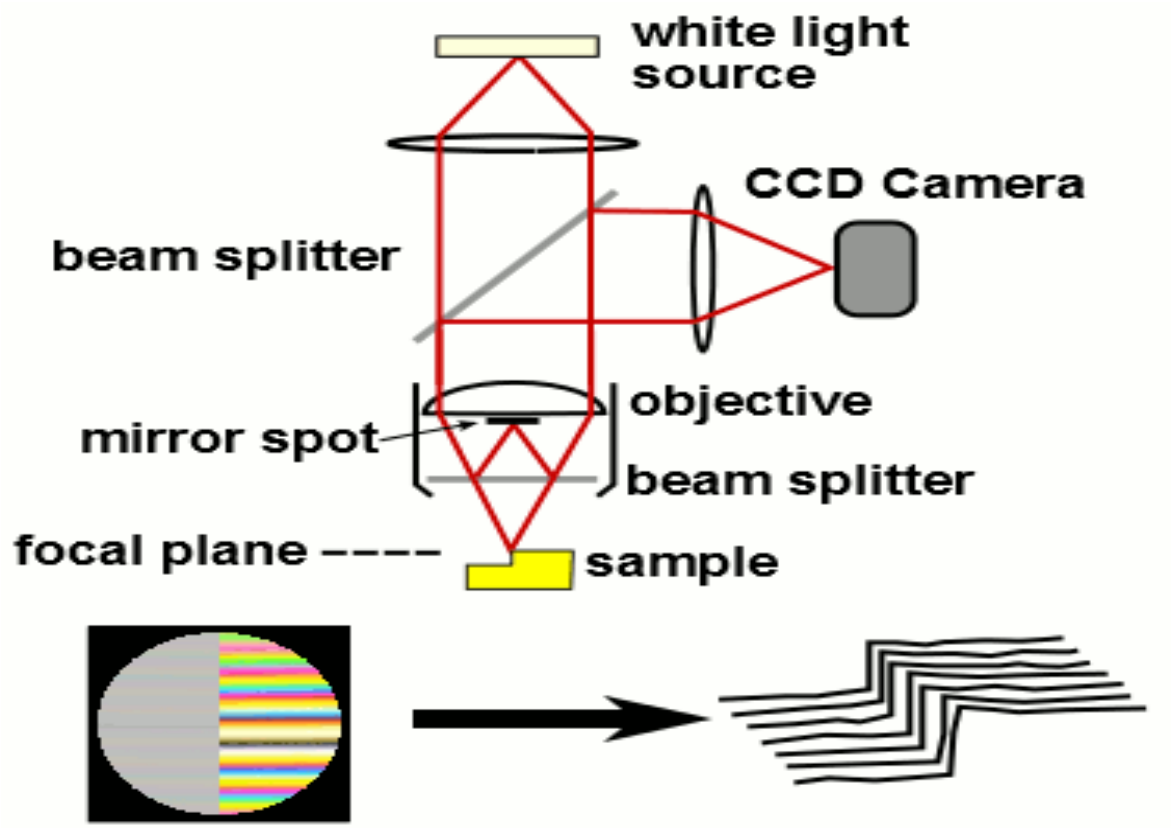

Figure 28: Working of white light scanners.

➢ Working

White-light interferometry scanning (WLS) systems capture intensity data at a series of positions along the vertical axis, determining where the surface is located by using the shape of the white-light interferogram, the localized phase of the interferogram, or a combination of both shape and phase. The white light interferogram actually consists of the superposition of fringes generated by multiple wavelengths, obtaining peak fringe contrast as a function of scan position, that is, the red portion of the object beam interferes with the red portion of the reference beam, the blue interferes with the blue, and so forth. In a WLS system, an imaging interferometer is vertically scanned to vary the optical path difference. During this process, a series of interference patterns are formed at each pixel in the instrument field of view. This results in an interference function, with interference varying as a function of optical path difference. The data are stored digitally and processed in a variety of ways depending on the system manufacturer, including being Fourier-transformed into frequency space, subject to cross-correlation methods, or analysis in the spatial domain.

If a Fourier transform is used, the original intensity data are expressed in terms of interference phase as a function of wavenumber. Wavenumber k is a representation of wavelength in the spatial frequency domain, defined by $k = 2\pi/\lambda$. If phase is plotted versus wavenumber, the slope of the function corresponds to the relative change in group-velocity optical path difference D_G by $D_h = D_G/2n_G$ where n_G is group-velocity index of refraction. If this calculation is performed for each pixel, a three-dimensional surface height map emerges from the data.

In the actual measuring process, the optical path difference is steadily increased by scanning the objective vertically using a precision mechanical stage or piezoelectric positioner. Interference data are captured at each step in the scan. In effect, an interferogram is captured as a function of vertical position for each pixel in the detector array. To sift through the large amount of data acquired over long scans, many different techniques can be employed. Most methods allow the instrument to reject raw data that do not exhibit sufficient signal-to-noise. The intensity data as a function of the optical path difference are processed and converted to height information of the sample

Figure 29: White light Scanner

➢ **Specifications:**

- Cameras 1.4 / 2.0 / 5.0 MP
- 3D Scanning area 55mm - 1545mm
- Point spacing 0.03 mm - 0.71mm
- Scanning principle Phase-shifting optical triangulation, twin cameras
- Triangulation angle 10°/ 25°
- Scanning distance 430 - 1,330mm
- Size 560 mm x 240 mm x 170 mm
- Weight 5kg
- Light source White LED
- Power AC 80 - 230 V / 50 - 60 Hz
- O/S Windows 7, 8

➢ **Parameter to consider while selecting a 3D Scanner**

1.) **Point Density**

One significant difference in white light scanner and laser scanner results is in point density. To illustrate this example, let's use the screw and crank from a deodorant bottle. You can see from this side-by-side comparison the difference in detail the scanners are able to obtain. This detail is obtained not by accuracy but by having points closer together.

If the goal of the scan were to capture data about the general size and dimensions without the intricate details of the screw and dial, the ROMER Arm and laser scanner will capture this general shape. If the goal of the scan is to reconstruct the dial exactly, the white light scanner has point spacing that is much closer and will record the dial with greater detail.

2.) Speed

When it comes to speed and efficiency of a scanner, laser scanners have the advantage of speed, due to the fact that they can do one sweep much more quickly than the multiple shots a white light scanner obtains. For example, the ROMER Absolute RS2 can scan 50,000 points wirelessly, with real-time exposure.

But with the next-generation cameras, electronics and processors now used, white light scanners can now obtain scan data containing over 8,000,000 points in an area as small as 30mm square and in as little as a few seconds. Due to this rapid scanning speed, white light scanners have been found to be incredibly useful in face scanning and body scanning applications, since people often find it difficult to stand still. However when many shots are required to cover the part in point's additional time is required.

3.) Accuracy

White light technology is capable of accuracies up to less than 0.001 of an inch in small volumes. Once the volume gets over roughly one foot cubed, the accuracies will match that of the laser scanner at roughly 0.003 of an inch.

Since each job is truly unique, your Exact Metrology rep will advise you on which type of scanning will achieve the greatest accuracy based on your project's volume.

4.) Cost

A white light scanner is typically more expensive than a laser scanner. While low-cost white light scanners are available, the data they obtain is typically not up to par with that obtained by the higher quality scanners. Therefore, if scan data provided by a laser scanner will meet the needs of a project, this is often the choice our clients go with. If scan data with greater detail is needed, then white light would be a better choice. You can talk with your Exact Metrology representative for a recommendation guaranteed to fit your requirements.

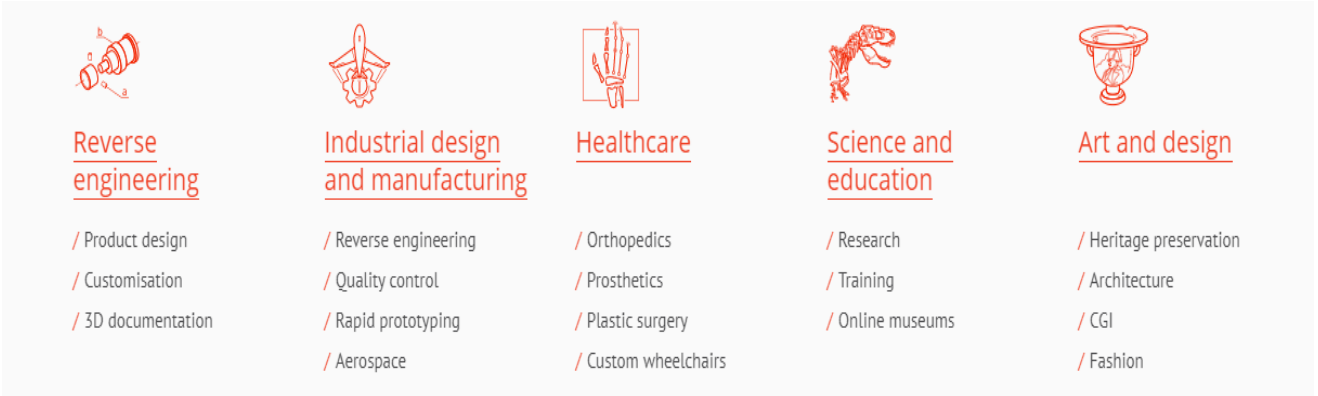

13. GEOMETRICAL EVALUATION

13.1 BENCHMARK MODEL

13.1.1 Experimental Procedure:

- A benchmark model is to be made on various platforms of different thickness.
- The orientation and position of the bench mark model (Fig Below) is to be kept constant as different platforms are used.
- After each build, the dimensions of the bench mark model are measured and the deviation from the nominal value is recorded.
- A plot of error v/s platform thickness is plotted to understand the nature of variation.
- The model is then subject to non-destructive testing for residual stress using X ray diffraction equipment to obtain the measurement of residual stress.
- The part quality is observed at the microstructural level for the presence of inclusions, porosities and cracks using optical microscope.
- The data is recorded and presented in an orderly fashion.

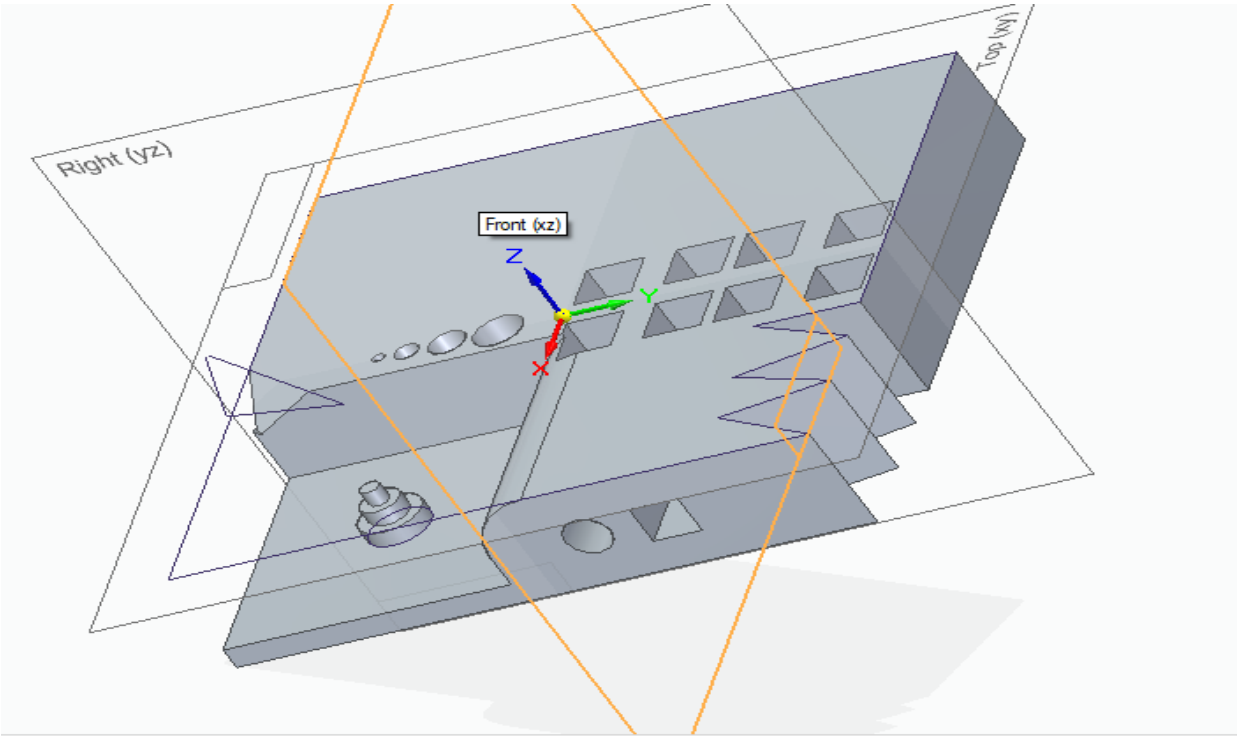

Figure 30 : 3D CAD model of becnchmark model

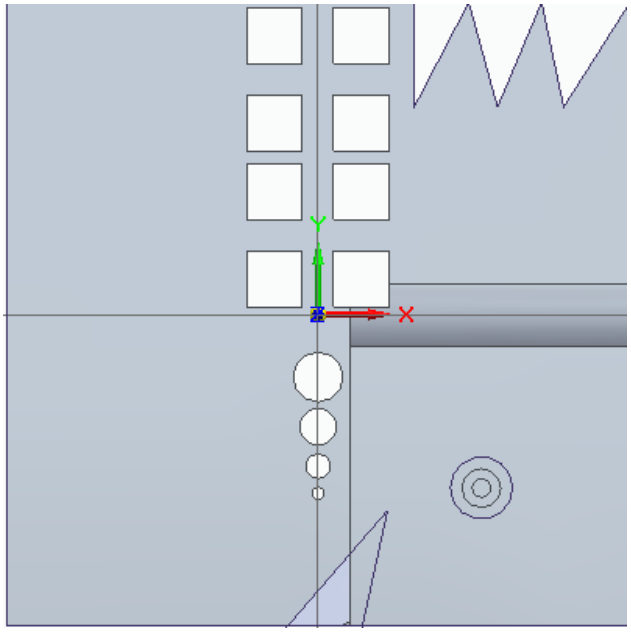

Top view

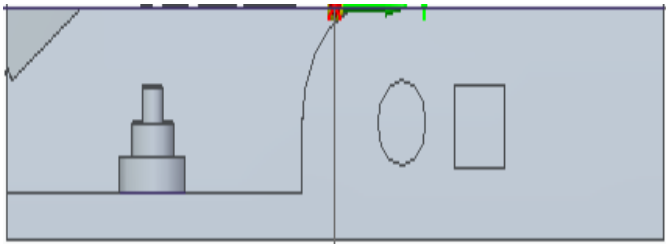

Side view

13.1.2 Available build Platforms:

1)Titanium Build Platforms (Machined)

PLATFORM NUMBER	THICKNESS(MM)	MASS(KG)
1	24.79	6.665
2	25.08	6.675
3	23.12	6.395
4	24.90	6.820
5	24.86	6.850
6	25.08	6.825
7	24.86	6.845
8	19.90	5.420
9	18.32	5.065
10	22.90	6.295
11	25.04	6.840
12	24.90	6.810

2) Stainless steel Build Platform used for Manufacture of Inconel:

PLATFORM NUMBER	THICKNESS(MM)	MASS(KG)
1	17.48	-
2	36.77	-
3	20.13	-
4	20.82	-
5	19.39	-
6	35.49	-
7	22.16	-
8	19.39	-
9	20.38	-

14.CONCLUSIONS

15.REFERENCES